DESIGN, SIMULATION, CONSTRUCTION AND PERFORMANCE EVALUATION OF A SOLAR BOX COOKER

BY

Abdulhamid ABDULLAHI

DEPARTMENT OF MECHANICAL ENGINEERING

FACULTY OF ENGINEERING

AHMADU BELLO UNIVERSITY,

ZARIA, NIGERIA

MAY, 2017

DESIGN, SIMULATION, CONSTRUCTION AND PERFORMANCE EVALUATION OF A SOLAR BOX COOKER

BY

Abdulhamid ABDULLAHI, B. Eng (ABU) 2013

P14EGME8013

A DISSERTATION SUBMITTED TO THE SCHOOL OF POSTGRADUATE STUDIES, AHMADU BELLO UNIVERSITY, ZARIA

IN PARTIAL FULFILLMENT OF THE REQUIREMENTS FOR THE AWARD OF A MASTER OF SCIENCE DEGREE IN MECHANICAL ENGINEERING

DEPARTMENT OF MECHANICAL ENGINEERING

FACULTY OF ENGINEERING

AHMADU BELLO UNIVERSITY,

ZARIA, NIGERIA

MAY, 2017

DECLARATION

I declare that the work in this dissertation entitled '**Design, simulation, construction and performance evaluation of a solar Box Cooker**' has been carried out by me in the **Department of Mechanical Engineering** under the supervision of Dr D.M. Kulla, and DrN.O. Omisanya. The information derived from the literature has been duly acknowledged in the text and a list of references provided. No part of this dissertation was previously presented for another degree or diploma in this or any other institution.

AbdulhamidABDULLAHI ……. …….....

Signature Date

CERTIFICATION

This dissertationentitled 'DESIGN, SIMULATION, CONSTRUCTION AND PERFORMANCE EVALUATION OF A SOLAR BOX COOKER'by ABDULHAMID ABDULLAHImeets the regulations governing the award of the degree of **Master of Science** in **Mechanical Engineering** of **Ahmadu Bello University,** and is approved for its contribution to knowledge and literary presentation.

Dr. D.M. Kulla _____ _____

(Chairman, Supervisory Committee) Signature Date

Dr. N.O. Omisanya _____ _____

(Member, Supervisory Committee) Signature Date

Dr. F.O. Anafi _____ _____

(Head of Department) Signature Date

Prof. A. Z. Abubakar _____ _____

(Dean, School of Postgraduate Studies) Signature Date

ACKNOWLEDGEMENTS

This dissertation would not have been possible without the support, guidance and encouragement of several individuals who, in one way or another contributed and extended valuable assistance in the preparation and completion of this study. First and foremost, i offer my sincere gratitude to my supervisors Dr D.M. Kulla and Dr N.O. Omisanya for their quality supervision, advice and guidance right from the very beginning of this research as well as giving me an extraordinary experience throughout this work. I am indeed much indebted to you for using your precious time to read through the dissertation and provide your critical comments. My special thanks go to the Head of Department Mechanical Engineering and all the staff of the department. I would like to acknowledge my elder brother Arc. AliyuAbdullahi and my Sister Hajiya Khadija Hassan Ibrahim for their support and encouragement. Also my appreciation to my friends and colleagues:

Muhammad Baba Abdullah, Dada Abdullah, Yakubu Umar Sanda, Engr. Abdullahi Mohammed and many others. My gratitude would not be completed without mentioning DevidHir Peter for his quality assistance and all the staff of Mechanical Engineering workshop for their valuable help during the construction process. Thank you all.

ABSTRACT

A solarbox cooker is a device that converts solar energy into useful heat in a confined space. The solar cooking system which captures and utilizes the abundant solar energy was designed, simulated, constructed and tested. Plane reflectors were used to concentrate solar radiations continuously on the collector which result to heat gain. It is usually difficult to manually track the movement of the sun and the use of a tracking device may be very expensive. Hence, plane reflectors were used. At the initial stage, the typical metrological year (TMY) solar data of Zaria obtained was processed to obtain the monthly average daily solar resources of Zaria using the solar radiation and weather data processor TYPE 109 component of TRNSYS 16 software. The month with the least average daily solar radiation was considered as the design month and the result shows that the month of August has the least solar radiation and therefore, considered as the design month.Secondly, the solar cooker was constructed at Ahmadu Bello University, Zaria Mechanical Engineering Workshop using various tools for cutting and machining.Thirdly, the solar cooker was tested at Mechanical Engineering Department of ABU between 28th and 31st of October, 2016. During the course of the testing, it was observed that in general the performance of the cooker was so encouraging because it cooked rice within an hour. The maximum stagnation temperature and that of absorber plate temperature were found to be 141^{o}C and 143^{o}C respectively. The cooker was simulated using TRNSYS and EES software. The simulated results were compared with the experimental results to determine the level of agreement between the two using Root Mean Square Error (RMSE) and Nash Sutcliff Efficiency (NSE) statistical tool. The RMSE results are 4.8203^{o}C and 2.604^{o}C. While the NSE results are 0.9867 and 0.996. These results show that the experimental values and the simulated values are in good fit.The regression line for the experiment and simulation were obtained and were used to compute the cooking power of the cooker. At 50^{o}C, the experimental and simulated cooking powers

are 52.8W and 54.8W respectively. For the average solar radiation incident on surfaces at different time intervals for the 4 conservative days, the regression line showing line of best fit for the co-efficient of determination (r^2) was found to be 91.87%. And also, for the variation of simulated and experimental collector efficiency, the co-efficient of determination (r^2) for both the simulated and experimental results were found to be 98.8% and 94.1% respectively. And the percentage of energy increment due to third reflector was found to be 84.5%

TABLE OF CONTENTS

TITLE PAGE i

DECLARATION ii

CERTIFICATION iii

ACKNOWLEDGEMENTS iv

ABSTRACT v

TABLE OF CONTENT vii

LIST OF FIGURES xii

LISTOFTABLES xiv

LIST OF APPENDICES xv

NOMENCLATURE xvi

CHAPTER ONE

INTRODUCTION.....1

1.1 Background 1

1.2 ProblemStatement.....3

1.3 Present Work.....3

1.4 Aim and Objectives.....4

1.5 Justification of the Work.....4

1.6 The Scope of the Study 5

CHAPTER TWO

LITERATUREREVIEW 6

2.1 Solar Energy and Its Application 6

2.2Solar Spectrum and Solar Constant.....7

2.3Solar Cookers and Their Types.....7

2.3.1 Working Principles of Solar Cookers 10

2.3.2 Advantages of Solar Cookers.....10

2.3.3 Disadvantages of Solar Cookers 11

2.3.4 Application of Solar Cookers.....11

2.4 Review of past works 12

2.4.1 Box solar cooker.....12

2.4.2 Parabolic solar cooker 4

2.4.3 Panel type solar cooker.....16

2.5 Actual Test Design Parameter (ASAE S580).....6

CHAPTER THREE

MATERIALS AND METHODS 18

3.1 Description of the solar cooker 18

3.2 Working principles 19

3.3 Materials 21

3.3.1 Materials selection 21

3.3.2 Measuring equipments for experimentation 22

3.4 Design considerations 23

3.5 Design theory.....23

3.5.1 Determination of design month 23

3.5.2 Solar angles.....24

3.5.2.1 Tilt angle 24

3.5.2.2 Declination.....25

3.5.2.3 Hour angle (w) 25

3.5.2.4 The azimuth angle (ϕ) 25

3.5.2.5 Zenith Angle (θ_z).....26

3.5.2.6 The optimum tilt angle for booster mirror 26

3.5.2.7 Solar Radiation Theoretical Background.....26

3.5.2.7.1 Incident radiation 26

3.5.2.7.2 Reflection of radiation 28

3.5.3 Energy analysis of solar cooker 28

3.5.3.1 Collector performance 28

3.5.3.2 Collector Efficiency.....29

3.5.3.3 Thermal efficiency.....29

3.5.4 Collector Dimensions.....30

3.5.4.1 Solar cooker surface collector area 30

3.5.4.2 Cooker wall insulation thickness 30

3.5.5 Stagnation temperature test.....31

3.5.6 Performance measures 32

3.6 Design Calculations.....34

3.7 Design of Reflectors 45

3.8 Solar Cooker Construction 48

3.9 Cost of the Solar Cooker 54

3.10 Solar Cooker Model.....56

3.11 Simulation of Performance 58

3.12 Simulation of solar cooking chamber temperature 59

3.13Modeling of Heat System.....59

3.14 Experimental Setup 61

3.15 Test Procedure 61

3.16 Error Analysis.....62

CHAPTER FOUR

RESULTS AND DISCUSSION 64

4.1 The Variation of Solar Insolation with time.....64

4.2 Design month.....65

4.3 Variations of Simulated and experimental collector efficiency 65

4.4 Results Generated from TRNSYS and EES modelling.....66

4.5 Comparison of simulated and experimental results 66

4.6 Error Analysis of the comparison between experimental and simulation results.....75

4.7 Validation of Simulated and the Experimental Results 81

4.8 Analysis of the predictive power of the simulation software (TRNSYS 16) and (EES 81

4.9 System performance measurement 82

CHAPTER FIVE

SUMMARY, CONCLUSIONS AND RECOMMENDATIONS 84

5.1 Summary.....84

5.2 Conclusions.....85

5.3 Recommendations.....85

REFERENCES.....86

APPENDICES.....92

LIST OF FIGURES

Figure 2.1: Panel Solar Cooker.....8

Figure 2.2: Box Solar Cooker.....9

Figure 2.3: Parabolic Solar Cooker.....10

Figure 3.1: Pictorial view of the three reflectors solar box cooker.....19

Figure 3.2: Modelling of Solar Cooking Chamber.....56

Figure 3.3: TRNSYS Simulation Model.....61

Figure 4.1: Variation of Average Solar Intensity with time from 28/10/2016 to 31/10/2016 64

Figure 4.2: Solar radiation and ambient temperature variation for 16th August for Zaria.....65

Figure 4.3: Variation of efficiency on the collector surface over time difference for simulation and experimental results.....66

Figure 4.4: Experimental and simulated incident solar radiation with local time (28th October, 2016).....67

Figure 4.5: Experimental and simulated stagnation temperature with local time (28th October, 2016).....68

Figure 4.6: Experimental and simulated ambient temperature with local time (28th October, 2016).....69

Figure 4.7: Experimental and simulated incident solar radiation with local time (30th October, 2016).....70

Figure 4.8: Experimental and simulation water temperature with local time (30th October, 2016) 72

Figure 4.9: Experimental and simulation ambient temperature with local time (30th October, 2016) 73

Figure 4.10: Experimental and simulated incident solar radiation with local time (31th October, 2016) 74

Figure 4.11: Experimental and simulated water temperature with local time (31th October, 2016) 74

Figure 4.12: Experimental and simulated ambient temperature with local time (31th October, 2016) 75

Figure 4.13: Adjusted cooking power plotted over temperature difference and resulting regression line for experimental results (30th October, 2016) 82

Figure 4.14: Adjusted cooking power plotted over temperature difference and resulting regression line for simulation results (30th October, 2016) 82

LIST OF TABLES

Table 3.1: Recommended Average Days for months and Values of n_i (Day of theYear) by months 24

Table 3.2: Construction Process for Solar Cooker.....48

Table 3.3: Costs analysis for the Solar Cooker.....54

Table 3.4: Simulation parameters for solar box cooker model.....60

Table 4.1: simulated result with experimental result of 30th October, 2016 using RMSE and NSE.....76

Table 4.2: simulated result with experimental result for 31th October, 2016 using RMSE and NSE.....78

LIST OF APPENDICES

Appendix A 92

Appendix B 94

Appendix C 96

Appendix D 99

Appendix E 104

Appendix F 107

NOMENCLATURE

A_a Aperture area of collector cavity (m^2)

A_i Area of inside cavity (m^2)

A_{sc} Surface collector area (m^2)

bCollector breadth

C_wSpecific heat capacity of water (j/kgk)

F_{ta}Product of the transmissivity of the glazing and the absorptivity of the absorber plate

F_1First figure of merit

F_2Second figure of merit

h_r Linear radiation heat transfer co-efficient ($w/m^{2o}C$)

h_1Convection heat transfer coefficient of air to glass cover

h_2Convection heat transfer coefficient of air to base of collector

h_3Convection heat transfer coefficient of air to sides of collector

h_{pt}Convection heat transfer coefficient of air to pot

h_tConvection heat transfer coefficient of air to tray

h_wWind Convection coefficient

h_{rca}Radiation heat transfer coefficient from glass cover to air

H_{tg1} Highest top distance of the absorber plate to the outer glazing

h_{tg1}Lowest top distance of the absorber plate to the outer glazing

H_{bg2}Highest bottom distance of absorber plate to the inner glazing

h_{bg2} Lowest bottom distance of absorber plate to the inner glazing

I_{av}Average solar insolation (W/m^2)

I_bBeam radiation on a horizontal surface (W/m^2)

I_{bc}Beam component of solar radiation on collector (W/m^2)

I_{dc}Diffuse component of solar radiation on collector (W/m^2)

I_dDiffuse radiation on a horizontal surface (W/m^2)

I_rReflected radiation (W/m^2)

I_TGlobal radiation (W/m^2)

I_τTransmitted radiation (W/m^2)

I_{bT}Beam radiation on tilted surface (W/m^2)

I_{dT}Diffuse radiation on tilted surface (W/m^2)

k_aThermal conductivity of air (W/m^{o}C)

k_wThermal conductivity of water (W/m^{o}C)

K_{pt} Thermal conductivity of pot (kJ/h m ^{o}C)

M_w Mass of water (kg)

N_uNusselt number.

Nu_1 Nusselt number of air on horizontal sides

Nu_2 Nusselt number of air on vertical sides

P_c Cooking power (Watt)

P_s Standardised cooking power (Watt)

Q_a Absorbed energy (W/m^2)

Q_u Rate of useful heat energy extracted from the collector (W/m^2)

q_u Useful energy gain (J/m^2)

R Rayleigh number

R_b Geometrical ratio

Ra_1 Rayleigh number of air on horizontal sides

Ra_2 Rayleigh number of air on vertical sides

SST Standardised stagnation temperature (^{o}C)

S_{rc} Shading factor on the collector due to the third reflector

T_{am} Ambient temperature (^{o}C)

T_{ap} Absorber plate temperature (^{o}C)

T_m Mean temperature (^{o}C)

T_{bo} Boiling point of water temperature (^{o}C)

T_d Temperature difference between that of water and ambient one (^{o}C)

T_{Dsim} Temperature difference for simulation (^{o}C)

T_{Dexp} Temperature difference for experimental (^{o}C)

T_f Final temperature of water (^{o}C)

T_i Initial temperature of water (^{o}C)

T_{io} Temperature of oven chamber (°C)

T_o Stagnation temperature (^{o}C)

T_w Temperature of water (^{o}C)

T_{g1} Outer glass temperature (^{o}C)

T_{g2} Outer glass temperature (^{o}C)

U_L Heat transfer co-efficient (W/m^{2o}C)

U_{sb} Bottom and side loss co-efficient (W/m^{2o}C)

V_{am} Ambient air velocity in (m/s)

$\dot{V}_{av}$ Average volumetric flow rate in glazing 1 and 2

Greek Symbols

θ_i Angle of incidence of beam radiation

θ_z Zenith angle of the sun

β Angle of inclination

β_c Tilt angle of collector

β_{opt} Optimum collector slope

Azimuth angle

γ_sSurface azimuth angle

δ Angle of declination of the sun

φ Angle of latitude

ω Hour angle

ρ Reflectivity

ε_c Emittance of glass cover

τ Transmisivity of glass cover

τ_d Transmitance of glazing for diffuse radiation

α_i Absorptance for diffuse radiation

α_{eff} Effective absorptance

$(\tau\alpha)_{bc}$ Transmittance – absorptance product of beam radiation

$(\tau\alpha)_{dc}$ Transmittance – absorptance product of diffuse radiation

σStephen-Boltzman constant

η_u Thermal efficiency

η_c Collector Efficiency

$\dot{m}$ Mass flow rate (Kg/s)

β_{r1} Tilt angle of reflector R1.

β_{r2} Tilt angle of reflector R2.

β_{r3} Tilt angle of reflector R3.

β_c Collector tilt angle.

θ_{r1} Angle of incidence of solar radiation on R1.

θ_{r2} Angle of incidence of solar radiation on R2.

θ_{r3} Angle of incidence of solar radiation on R3.

CHAPTER ONE

INTRODUCTION

1.1 Background to the Study

Energy is a thermodynamic quantity which is described as the capacity of a physical system to do work. Energy is vital for our relations with the environment, and thus the research to resolve problems related to energy is quite significant since life is directly affected by energy and its consumption. Fossil fuel based energy resources still predominate with the highest share in global energy consumption (Chinnumol and Victor, 2015). An enormous amount of energy is thus expended regularly on cooking. In almost all the rural homes and many urban homes in Nigeria, the traditional and most popular source of energy for cooking is firewood (Kulla, 2011). The projected wood consumption in Nigeria for the year 2000 was 23.6 million tonnes of oil equivalent (Ekechukwu and Abdussalam, 2001).

Desert encroachment and global warming are few among many resultant effects. Most urban dwellers also use kerosene and other petroleum bye products for cooking amidst its attendant environmental hazards. Fossil fuels are not environmentally friendly owing to emissions arising from bye products of combustion which constitute health hazards (Basil, 2013). The energy required for cooking is supplied by non-commercial fuels like firewood, agricultural waste, cow dung and kerosene (Erdem and Pinar, 2013).

Nigeria is blessed with a significant level of solar insolation. The country receives about 5.08 x 10^{12} KWh of energy per day from the sun (Aremu and Akinoso, 2013). The technology of solar cooking involves the conversion of solar energy to heat energy. The heat is then directed to cooking pot for food preparation. Solar cooking systems could be box type, concentrating type or a hybrid of the two. Box-type solar cooker makes use of both diffuse and direct radiation while the concentrating type depends on its ability to make use of direct radiation only (Aremu and Akinoso, 2013).

Solar energy is one of the main alternative renewable sources of energy crucial to our search for domestic fuel replacements. This is because; it is the source of almost all renewable and non-renewable sources of energy. Also, it is the cleanest, free from environmental hazards and it is readily available and inexhaustible (Bello *et al.*, 2010).

Solar energy presents an alternative energy source for cooking, which is simple, safe and convenient without consuming fuels and polluting the environment. It is appropriate for

Hundreds of millions of people around the world with scarce fuel and financial resource to pay for cooking fuel (Chinnumol and Victor, 2015). Solar cookers can also be used for boiling of drinking water, providing access to safe drinking water to millions of people thus preventing water-borne illnesses (Chinnumol and Victor, 2015).

Solar cookers are heat exchangers designed to use solar energy in cooking process (Haftom*et al.*, 2014). In supplying the needed energy, solar cookers can fully or partially replace the use of firewood for cooking in many developing countries (Haftom*et al.*, 2014).Cooking is the art, technology and craft of preparing food for consumption with the use of heat. Cooking techniques and ingredients vary widely across the world, from grilling food over an open fire to using electric stoves, to baking in various types of ovens, reflecting unique environmental, economic and cultural traditions and trends (SC, 2016).

Solar cooking is the simplest, safest, most convenient way to cook food without consuming fuel or heating up kitchen. Many people choose to solar cook for these reasons. But for hundreds of millions of people around the world who cook over fires fuelled by wood or dungs, and who walk miles to collect fire wood or spend much of their meagre income on fuel, solar cooking is more than a choice-It is a blessing (SC, 2016).

1.2 Problem Statement

Cooking using firewood has led to wood shortages (Aremu and Akinoso, 2013).In meeting the essential and basic need of human being, wood and fossil fuel as sources of energy for cooking food have played tremendous and invaluable roles. However, the direct combustion of wood and fossil fuel as the major sources of cooking has immensely contributed to global warming and acid rains (Sobamowa*et al*., 2012). Aside from these adverse effects of global warming, the inhalation of these gases irritates the lungs and the eyes and can cause diseases such as pneumonia (Sobamowa*et al*., 2012).

Electric cookers are also source of heat energy. But unfortunately the high cost of electric energy generation and distribution added to erratic power supply, which constitute obvious drawbacks. Nigeria as well as other countries in the tropics is readily blessed with abundant supply of solar energy which can conveniently be harnessed to fill this gap (Basil, 2013). About two billion people are daily dependent on firewood as a source of their domestic and heating energy. They live in the tropics which are the most favourable area for harnessing solar energy (Ohajianya*et al.*, 2014). Therefore, there is need for developing solar stoves to harness the available solar energy. However, some solar cookers use only one reflector which results to low solar radiation. Therefore, the radiation can be improved by increasing the number of reflectors which result to high absorber plate temperature into the cooking chamber.

1.3 Present work

The present work is to design, simulate, construct and evaluate the performance of a box solar cooker using three reflectors. The Box solar cooker was built using three reflectors and plane mirrors were used to serve as booster of solar radiations to the cooking chamber. Ply wood was used to build the inner and outer casing and good insulating material (fibre glass) was inserted in between the casing to minimize heat loss. Double transparent glass (window

frame) on top of the cooker was served as top cover that let in sunlight. However, absorber plate was attached to the inner box casing and served as the cooking chamber were the cooking chamber was coated with matte black colour for better heat absorption. A mathematical model using TRNSYS simulation based programme and Engineering Equation Solver (EES) was used to simulate the components of the cooker to compare with constructed components.

1.4 Aim and objectives

The aim of the project is to design, simulate, fabricate and carry out the performance evaluation of box solar cooker using three plane reflectors to achieve cooking under Zaria metrological condition.

Specific objectives are to:

i. Carry out design analysis to determine the dimensions of solar cooking system.
ii. Simulate the design and evaluate performance of the collector under Zaria metrological condition
iii. Construct and carry out performance evaluation of the solar cooker.

1.5 Justifications

No petroleum, diesel or any artificial form of fuel required to use in solar cooker. But rather, it uses sunlight which is in abundant. Many profit organizations are promoting their use worldwide in order to help reduce fuel cost and to avoid air pollution. The use solar cooker in homes dramatically lead to decrease in illegal electrical connections and consequent fire outbreak. Solar cooking systems can operate for many years without requiring any serious maintenance. So therefore, very little service or maintenance is required for the life of the system. Solar cooker produces no waste products such as carbon dioxide or other chemical

pollutants, so has minimal negative impact to the environment. Use of solar energy slows down:

a. **Deforestation:** clearing earth's forest on a massive scale often resulting in damage in the quality of the land.
b. **Desertification**: process by which fertile land becomes desert, typically as a result of drought, deforestation and in appropriate agriculture.

The use of solar energy helps in reducing electricity consumption. The saved energy could be used for other activities (Mohammed, 2015).

1.6 The Scope of the Study

The work done covers the following areas:

a) Design and selection of materials at a specified dimension.
b) Simulation of the solar cooker.
c) Performance evaluation of the cooker.

CHAPTER TWO

LITERATURE REVIEW

2.1 Solar Energy and Its Application

Solar energy is the energy transmitted from the sun in the form of electromagnetic radiation, which requires no medium for its transmission. The earth receives about one – half of one billionth of the total solar output. Among all the nonconventional energies, solar energy is the best option if it can be used in a cost effective manner because the technology is also environmentally friendly. As the solar energy intercepted by the earth in one year is ten times greater than the total fossil resources including undiscovered and unexplored non-recoverable reserves (Medugu*et al*., 2013). It is expected that the present worldwide research and development program on solar energy will help to solve the future energy crisis of the world (Medugu*et al*., 2013). Solar radiation otherwise known as insolation is the amount of energy from the sun reaching a specific location on the surface of the earth at a specified time. Due to the interference of the atmosphere, solar energy hits a horizontal plane on earth in direct and diffuse forms. The direct form is the parallel rays from the direction of the sun while the diffuse forms is radiation scattered in many directions by matter and gases in the atmosphere. The diffuse radiation are caused by the reflection and scattering by the atmosphere (Ogbuisi, 2010).

The Application of Solar Energy is as follows:

a) Residential Application Use of solar energy for homes has number of advantages. The solar energy is used in residential homes for heating the water with the help of solar heater. The photovoltaic cell installed on the roof of the house collects the solar energy and is used to

warm the water. Solar energy can also be used to generate electricity. Batteries store energy captured in day time and supply power throughout the day. The use of solar appliances is one of the best ways to cut the expenditure on energy (www.solarpoweryourhouse.com, 2008).

b) Industrial Application Sun's thermal energy is used in office, warehouse and industry to supply power. Solar energy is used to power radio and TV stations. It is also used to supply power to lighthouse and warning light for aircraft (www.solarpoweryourhouse.com, 2008).

c) Remote Application Solar energy can be used for power generation in remotely situated places like schools, homes, clinics and buildings. Water pumps run on solar energy in remote areas. Large scale desalination plant also use power generated from solar energy instead of electricity (www.solarpoweryourhouse.com, 2008).

2.2 Solar Spectrum and Solar Constant

The distribution of solar radiation as a function of the wavelength is called the solar spectrum, which consists of a continuous emission with some superimposed line structures. The Sun's total radiation output is approximately equivalent to that of a blackbody at 5776K. The solar radiation in the visible and infrared spectrum fits closely with the blackbody emission at this temperature. However, the ultraviolet (UV) region (<0.4 micrometer) of solar radiation deviates greatly from the visible and infrared regions in terms of the equivalent blackbody temperature of the sun. In the interval 0.1–0.4 micrometer, the equivalent blackbody temperature of the sun is generally less than 5776K with a minimum of about 4500K about 0.16 micrometer (Goody and Hu, 2003). The deviations seen in the solar spectrum are result in emission from the non isothermal solar atmosphere (Goody and Hu, 2003).

2.3 Solar Cookers and Their Types

Solar cookers are devices that cook food using only solar radiation and can save conventional fuels to a significant amount. It is the simplest, safest, most convenient way to cook food

without consuming fuels or heating up the kitchen (Mohammed, 2015). Several factors including access to materials, availability of traditional cooking fuels, climate, food preferences, and technical capabilities affect people's perception of solar cooking (Ismail and Isah, 2013).

Types of Solar Cookers

There are three types of solar cookers:

- Panel Solar Cooker
- Box Solar Cooker
- Parabolic Solar Cooker

a) Panel Solar Cooker

Figure 2.1 is the pictorial view of a panel solar cooker. The panel cooker is the least expensive type of solar cooker. It is designed to reflect sunlight over the entire surface of a lightweight. Cooking pot is said to be coated with black colour on the outside with non-toxic paint. They are unstable in high winds and do not retain as much heat when the sun is hidden behind the clouds (SCP, 2015)

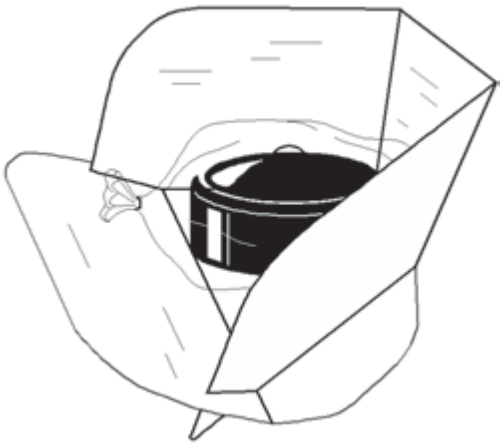


Figure 2.1: Panel Solar Cooker (SCP, 2015)

b) Box Solar Cooker

Figure 2.2 is the pictorial view of a box solar cooker. Solar box cookers (sometimes called solar ovens) are the most common and inexpensive type of solar cookers. This type of solar

cooker consists of an insulated box made of cardboard, wood, metal or plastic.It is painted black on the inside and has a large glass or Plexiglas window on top to let in sunlight. Just like panel cookers, box cookers can be left unattended in the sun for hours to cookfood and pasteurize water. There is no danger of burning the food. Box solar cookers only need a slight adjustment to track the sun every few hours. Some solar box cookers have aluminium reflectors on the outside to direct even more sunlight into the box (SCP, 2015).

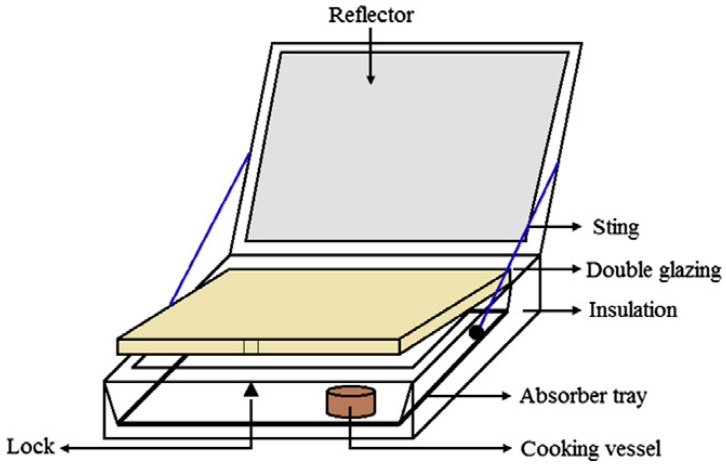


Figure 2.2: Box Solar Cooker (Erdem and Pinar, 2013)

c) Parabolic Solar Cooker

Figure 2.3 is the pictorial view of a parabolic solar cooker. Parabolic solar cookers operate at a much higher temperature than panel and box cookers. They focus a narrow beam of sunlight on to the bottom of a cooking pot that sits on a metal stand. Although parabolic solar cookers require regular adjustments to track the movement of the sun, they can be used from sunrise to sunset (SCP, 2015).

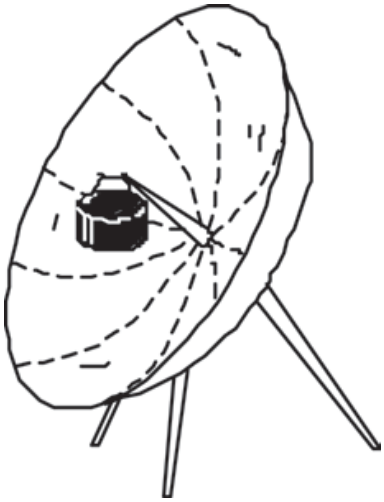


Figure 2.3: Parabolic Solar Cooker (SCP, 2015)

2.3.1 Working Principles of Solar Cookers

Sunlight to heat conversion occurs when photons (particles of light) moves around in a substances. The rays emitted by the sun have a lot of energy in them when they strike matter. Whether solid or liquid, all of this energy causes the molecules in that matter to vibrate. They get excited and start jumping around. The activity generates heat (SCP, 2015).

2.3.2 Advantages of Solar Cookers

The biggest advantage of solar cookers is eco-friendliness. By using one, dependency on gas or electricity can be gone. Better air quality indoors can be maintained, reduce carbon monoxide emission, enjoy cooler temperatures indoors and conserve more fuel by reducing the need for air conditioning. Solar cookers are free, once you have the cooker itself. To operate one, all to be needed is sunlight; significant amount of money can be save over a long term. As a result, solar cookers are being used increasingly in different parts of the world, especially in poorer communities with limited access to fuel and power since it is very simple to build one from scratch.

2.3.3 Disadvantages of Solar Cookers

Cooking with solar cookers obviously requires sunlight, which makes it difficult to use during winter months and on rainy days. Cooking also takes significantly longer time compared with conventional method. Users must schedule their cooking time and maximize the use of sunlight. As a result, preparation must start early in the morning so that food can be placed in the cooker by noon. Solar cookers are not as efficient at retaining heat as conventional cooking devices. Factors such as wind, rain and snow can seriously hinder operation, and in such weather conditions, even after the food is cooked, it will lose its warmth very quickly.

2.3.4 Application of Solar Cookers

i. **Canning fruits and tomatoes:** In a solar oven (only fruits and highly acidic items like tomatoes can be canned using solar ovens). But, pressure cooker can be used on a large parabolic cooker to pressure can, due to high heat concentration. Of course, the cooker has to be rig to withstand a large amount of weight (www.solarcooker-continawest.com, 2013).

ii. **Dehydration of food:** This can be done on a solar box cooker (oven) by ventilating the interior of the oven by leaving the door/lid partially open to prevent excess build up of heat and to allow air movement (www.solarcooker-continawest.com, 2013).

iii. **Water purification and pasteurization:** Solar cooker are used for purification and pasteurization around the world, especially when the water is polluted and needs purification (www.solarcooker-continawest.com, 2013).

iv. **Grain sterilization:** Can be accomplished in a solar oven to kill weevil and other bugs (www.solarcooker-continawest.com, 2013).

v. **Medical instrument sterilization:** Doctors in third-world countries have used solar ovens and panel style cookers to sterilize their medical instruments, gauge bandages

and needles to help reduce and prevents the spread of infections (www.solarcooker-continawest.com, 2013).

2.4 Review of past works

A number of researches have over the years been carried out on solar cooking system.

2.4.1 Box solar cooker

Theoretical and experimental comparism of box solar cookers with and without internal reflector was carried out by Mulu*et al*., (2013). The study has clearly shown that in both the theoretical prediction and experimental tests, the performance of box solar cookers can be enhanced using internal reflectors. The steady state theoretical analysis predicted difference in standard stagnation temperature of about 25^{o}C. The experiment on stagnation test also concluded that the standard stagnation temperature was higher by about 22^{o}C. However, the predicted stagnation temperature for both the cookers was higher than the experimental value. Similarly the boiling test indicated that the water temperature and the cumulative efficiency were higher for the cooker with reflector.

The performance, modelling and parametric analysis of a solar oven was carried out by Abdulwahid*et al*., (2015). Experiments were conducted on the solar oven with and without reflectors and with a unique five sided double glazed painted with black. It was found that there was increased in radiation for a single glazed solar oven compared with the solar oven without glazing. Also for single glazed, thus absorbs more heat and losses more heat as well which resulted in low temperature than for double glazed due to the surrounding effects. It was found that the estimated average efficiency of the solar box cooker was found to be about 47.56%.

The design, construction and performance evaluation of solar cookers was carried out by Elamin and Abdalla (2015). Saw dust was used as an insulator with a thickness of 5cm and placed at the bottom between collector and the thickness container. The result shows that the absorber plate temperature increased towards noon period then decreased towards evening. It shows that the maximum absorber plate temperature was found to be 127^0C.

The flat plate collector solar cooker was carried out by Ogunwole (2006). The black plate for heat absorption was fixed to the bottom of the inner layer of the casing. The dimension was 535mm by 535mm. Surface area of the board was 865mm by 865mm. the angle of inclination to the horizontal was found to be 72°.

The performance test and thermal efficiency evaluation of a constructed solar cooker at a guinea savannah station (Ilorin, Nigeria) was carried out by Bello *et al*. (2010). The trapezoidal shaped inner box of dimension 30cm by 30cm by 20cm bounded by an outer box measuring 80cm by 60cm by 30cm was designed. During the test, the maximum temperature was found to be 88°C.

The model solar box cooker designed for rural household energy needs was carried out by Fumen*et al*. (2014). A solar box with a wooden frame consisting of an insulated box, transparent glass covers, a reflective glass, an absorber plate and aluminium pots was constructed. It was concluded that the average heating temperature of the solar cooker was 77°C and the heat absorption rate of the heating water was 280kJ at each time interval. Also the maximum temperature of heated water was found to be 82°C.

The performance evaluation of a box-type solar oven with reflector was carried out by Yusuf *et al*. (2014). The solar oven was constructed with locally available materials. Plywood for casing, a 2 by 3 reflective mirror, metal, hinges, screw, black paint, 2 by 3 reflective plane

glass and insulator form were used. During the stagnation test, it was observed that the plate temperature at the bottom of the solar oven was found to be 110.2°C.

The energetic and exegetics evaluation box-type solar cookers using different insulation materials were carried out by Ademola and Joseph (2015). Five flat plate collectors type box cookers were designed and fabricated. The main distinguishing factors in the five cookers were the insulating materials used. The cookers were labelled 1-5 according to the insulation materials which were: maize cob, air (control), maize husk, coconut coir and polyurethane foam. 1.5 litres of water was loaded into the pots of each cooker. Energy andexergy analysis were carried out for the five box solar cookers with different insulating materials. The result shows that; the solar cooker with air as an insulator performed poorly when compared to others.

2.4.2 Parabolic solar cooker

The performance evaluation of a parabolic solar dish cooker in Yola, Nigeria was carried out by Aiden (2014). The dish collector was made from 0.7mm thick aluminium sheet. Iron bars were used to create supports for the dish and the pot. The manual sun tracking mechanism made from iron bars was also incorporated to constantly adjust the cooker to the sun's direction. The optical efficiency of the collector was found to be about 17.86%, the overall heat loss co-efficient of 8.896$Wk^{-1}m^{-1}$ and the adjusted cooking power that measured its performance was 96.53Watt.

The design and development of a parabolic dish solar thermal cooker was carried out by Ibrahim (2013). The parabolic dish solar thermal cooker having aperture diameter 1.8m, depth 29.0cm and focal length 69.8cm was design and constructed. The cooker was designed to cook food equivalent to 12kg of dry rice per day, for a relatively medium size family. The

preliminarily test results show the cooker was capable of cooking 3.0kg of rice in about 90-100 min.

The design and fabrication of manually track parabolic solar disc for in-house cooking was carried out by Suple and Suraskar (2012). In this fabrication work, a primary reflecting parabolic surface concentrates the solar radiation on it and reflects them on to the secondary reflectors. The secondary reflector then focused the incident radiation at the point of interest, thus generated heat used for cooking purposes.

The experimental investigation of heat losses from a parabolic concentrator solar cooker were carried out by Dasin (2013). The research records the experimental investigations of the cooker, which includes: the absorber (cooking pot), cooking pot cover and air contained in the cooking pot. Convective heat losses were important determining factor in the performance of this type of cookers. It was concluded that convective heat transfer losses was high for such type of cooker.

The performance test of a parabolic trough solar cooker for indoor cooking was carried out by Haftone*t al*. (2014). Parabolic trough cooker was constructed in a way allowing cooking to be done indoors, which the cooking sections were placed indoor while the collector parts out-door with soya beans oil conveying the energy from the absorber to the cooking stove. Ray tracing and standard stagnation tests showed a 30mm diameter copper pipe were optimized for the absorber. Maximum temperatures of 191°C at the mid absorber pipe and 119°C at the cooking stove were obtained. The efficiency of the system was found to be 6%.

The cylindrical solar cooker with automatic two axes sun tracking system was carried out by Essam*et al*., (2010). In this work, a cylindrical solar cooker with two axes sun tracking and another for rotating around vertical axes was designed. The programming method of control with open loop system was employed. Programmable logic controller was mounted. The test

showed that using cylindrical solar cooker system with two axes tracking can increase water temperature up to 90°C.

2.4.3 Panel type solar cooker

The development and evaluation of multi-reflector foldable type solar cooker was carried out by Mohod and Powar (2011). The base plate was made with cardboard(40cm by 40cm) pasted with 3mm thermocol sheet on the bottom reverse side and was used to hold the side walls of the cooker and to act as an insulator. It was found that the multi reflector foldable box type solar cooker provides the availability of cooking energy in the household. Also the figure of merit F_1=0.093 and F_2=0.232

2.5 Actual Test Design Parameter (ASAE S580)

The New World Standard Solar Cooker Test Procedure ''ASAE S580''

The actual testing of the working performance of the oven in operation was obtained using the ASAE (An international standard for testing solar cooker whose recommendations were accepted by the United State of Agricultural Engineers as ASAE S580).

The average temperature (^{0}C) inside a container of water was measured and averaged over ten minutes interval. Ambient temperature and normal irradiance were also measured and recorded. The primary figure of merit used in the ASAE standard is the cooking power, P_c defined by (ASAE S580, 2013)

$$P_c = \frac{M_w C_w (T_f - T_i)}{600} \qquad (2.1)$$

Where;

T_f= is the water temperature at the end of 10min interval initial temperature.

T_i= Initial temperature of the water

The cooking power was normalised for solar radiation of 700W/m^2 as (ASAE S580, 2013)

$$P_s = \frac{700Pc}{I_{av}} \quad (2.2)$$

The ambient temperature for each interval was subtracted from the average cooking vessel contents temperature for each corresponding interval

$$T_d = T_w - T_{am} \quad (2.3)$$

T_d= is the temperature difference

T_w= is the cooking vessels contents (water) temperature

T_{am}= is the ambient air temperature. All in (^{o}C)

The standardised Cooking power, P_s was plotted against temperature difference, T_d for each time interval.

A linear regression of the plotted points were used to find the relationship between cooking power and temperature difference in terms of intercept a (w) and slope b (W/^{o}C) given as (ASAE S580, 2013).

$$P_s = a + bT_d \quad (2.4)$$

CHAPTER THREE

MATERIALS AND METHODS

3.1 Description of the solar cooker

The system consists of an insulating material (fibre glass) in between theinner and outer casing to minimize heatloss. The casings were made with ply wood to further minimize heat loss and to serve as barrier to prevent any environmental effect to the solar cooker.An angle iron helps in tilting the two opposite small size reflectors and the big sized reflector is fixed which helps the two opposite small size reflector in boosting the solar radiations into the cooking chamber. The reflector handle is used in opening and closing the cooker when out of use as shown in figure 3.1. Inside the cooking chamber is an aluminium plate coated with a non toxic matte black colour to achieve high absorption coefficient. The cooking pot is situated 40mm above the bottom absorber plate. Light rays inpinging on the system are two: direct and reflected rays. Direct rays come directly from the sun into the cooking chamber through the glazing while the reflected rays hit the reflector and the reflected back to the cooking chamber through the glazing.

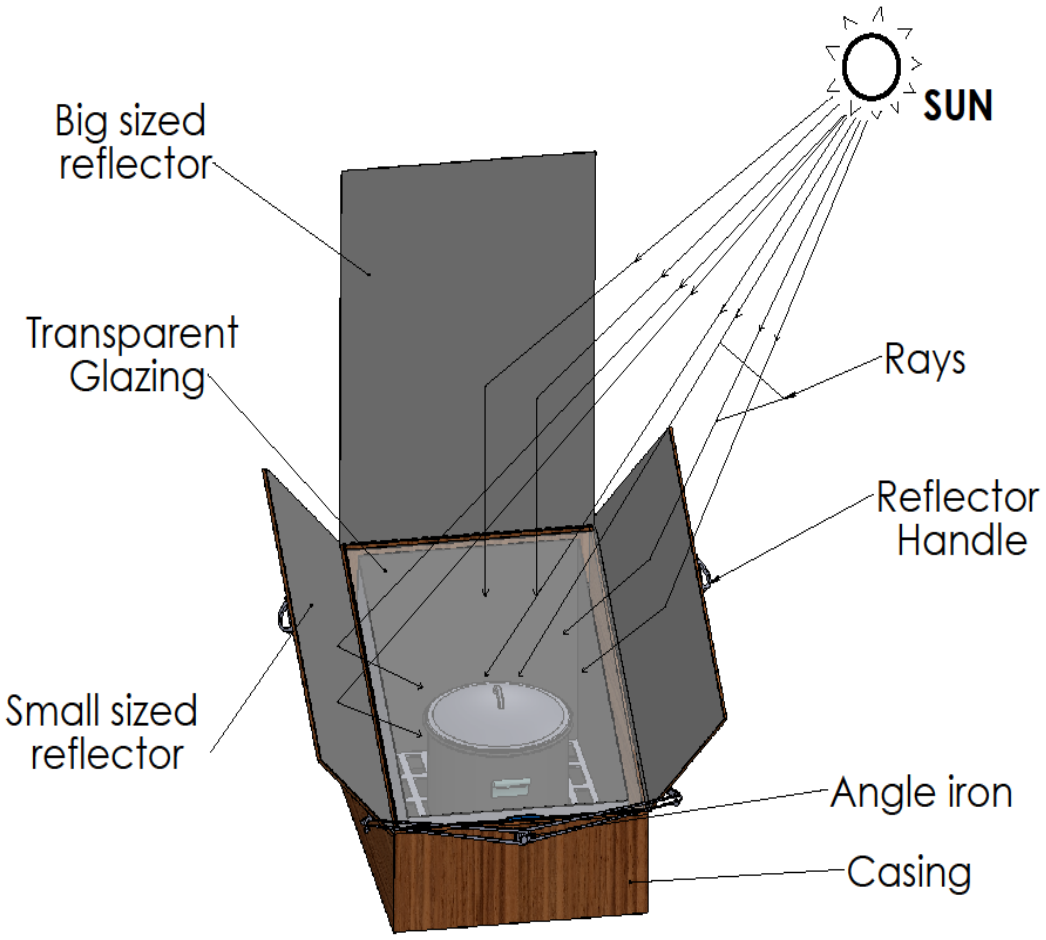


Figure 3.1: Pictorial view of the three reflectors solar box cooker

3.2 Working principles

Figure 3.1 shows a pictorial view of the three reflectors box solar cooker. Sunlight both direct and reflected enters the solar box through the glazing and turns to heat energy when absorbed by the dark absorber plate and cooking pot. This heat input causes the temperature inside of the solar cooker to rise which result to solar heat gain. Temperature sufficient for cooking food and pasteurizing water are easily achieved through this means.

The solar cooker consists of the following components:

i. **Reflectors**: Reflectors were employed to reflect more solar rate onto the absorber plate so as to increase the cooking temperature. And three reflectors were used.

ii. **Casing**: Inner and outer casing were used in housing the entire solar cooker with the exception of the window frame. It also contributed in minimizing heat loss to the surrounding.

iii. **Glazing (Window frame)**: Transparent glass was used to trap solar energy or hot air and to prevent wind from blowing over the cooking pot and also increased the efficiency of cooking.

iv. **Absorber plate (cooking chamber)**: Absorber plates was used to absorb sunlight and converted it to heat energy. To enhance such absorption, the plate was coated with matt black, because black body is a good absorber of heat.

v. **Insulators**: Insulators are materials that minimize heat loss and must be poor conductor of heat. And also used to fill the air space between the outer and the inner casing of the cooker.

vi. **Angle iron**: Angle is a metallic component that was used to hold the two reflectors in place and also help in varying the tilt angle to manually track the movement of sunlight.

3.3 Materials

3.3.1 Materials selection

i**. Reflectors**: In selecting the reflector for the solar cooker, plane reflector was used due to its high reflectance and low cost. Each reflector was attached to ply wood frame to hold the reflector in place.

ii. **Outer and inner casing:** Materials for casing includes; aluminium, fibre sheet, wood and galvanized iron. These materials have very well weather stability as well as durability, but differ in cost and weight. Ply wood was selected due to its; Low heat conductivity, Surface dimensional stability, High strength to weight ratio, Chemical resistance (www.woodsolution.com, 2016).

iii. **Glazing**: Glass and plastics are materials that were used in glazing. Transparent glass was selected due to its; material strength, durability, non-degradability when exposed to UV light and provision of heating through green house effect.

Glazing performs the following functions (Lefthriotis and Yianoulis, 2012):

i. Serves as a shield to the absorber plate from outside the environment.
ii. Minimize heat loss by convection and radiation from the absorber plates
iii. Transmit direct and diffuse solar radiation to the absorber plate with minimum loss.

Other features of glazing are reflection(r), transmission (T) and absorption (α)

The purpose of using glass cover is because it is highly effective in reducing heat loss from the absorber plate. Also it can withstand high temperature than plastics.

iv. **Absorber plate (cooking chamber)**: It absorbs both direct and diffuse solar radiation from the window frame. Aluminium plate was selected due to its good thermal conductivity, durability, appearance, corrosion resistance.

v. **Insulation**: Insulating material are used to minimize heat loss. Materials that are available are of different varieties. They include fiber glass, plywood, expanded polystyrene, cork and polyurethane form. Selection of one of the insulation material was based on cost, durability and its effectiveness. Material with low thermal conductivity was selected for better performance.

Fibre glass was used as insulating material due to the following advantages; Low heat conduction, Low density, Good mechanical strength, Resistance to fire (www.wikipedia.com, 2017).

3.3.2 Measuring equipments for experimentation

The following measuring equipments were used:

i. Thermometer: This is a sensor for measuring temperature. This sensor consists of two dissimilar metal wires joined at one end and connected to a thermocouple thermometer or other thermocouple-capable device at the other end. When properly configured, thermocouple can provide temperature measurements over wide range of temperatures (KM330 model).

ii. Weighing scale: Are devices used in measuring weight (3D model STL-Finder).

iii. Solarimeter: is a pyranometer, a type of measuring device used to measure combined direct and diffuse solar radiations. Integrating solarimeter measures energy developed from

solar radiation based on the absorption of heat by a black body (KIMO Solarimeter SL100-Kleinschm).

3.4 Design considerations

The considerations put in place in the design of box solar cooker are resistance to environmental condition and portability such that it could be transported easily without much difficulty. The cooker should be able to withstand thermal and mechanical stress for long period of time. It should be able to cook food materials such as yam, rice and also boiling of water for sterilization activities. Also, orientation of reflectors is another important consideration in the design because the collector efficiency depends on the solar radiations diffusing into the cooking chamber of the cooker.

3.5 Design theory

Radiation is available in form of daily and hourly on a horizontal surface. Using TRNSYS package, hourly radiation was generated from typical metrological year (TMY). TMY is a collation of selected weather data for specific location. Metrological data includes solar radiation and ambient air temperature for the testing of Zaria latitude location was generated.

3.5.1 Determination of design month

The design month is the month with the lowest solar irradiance. It is set to know the least system performance. The weather condition for the recommended average day for the month was utilized. The recommended average day for each month of the year is given in Table 3.1.

Table 3.1: Recommended Average Days for months and Values of n_i (Day of theYear) by months

Month	**Date**	**n_i**	**Hours**
January	17	17	384 – 408
February	16	47	1104 – 1128
March	16	75	1824 – 1848
April	15	105	2496 – 2520
May	15	135	3216 – 3240
June	11	162	3864 – 3888
July	17	198	4728 – 4752
August	16	228	5448 – 5472
September	15	258	6168 – 6192
October	15	288	6888 – 6912
November	14	318	7608 – 7632
December	10	344	8256 – 8280

Source:(Duffie and Beckman, 2013).

3.5.2 Solar angles

3.5.2.1 Tilt angle

The solar energy received by a flat collector is maximum if the tilt angle of the collector to horizontal is such that:

$$\beta = \phi + 10^{o} \quad (3.1)$$

Where: β is the tilt angle

ϕ is the latitude of the location

3.5.2.2 Declination

Declination is the angular position of the sun at solar noon (i.e when the sun is on the local meridian) with respect to the plane of the equator (Duffie and Beckman, 2013).

$$\delta = 23.45\sin\left(360\frac{n+284}{365}\right) \quad (3.2)$$

Where, n= day of the year

3.5.2.3 Hour angle (w)

Hour angle is the angular displacement of the sun east or west of the local meridian due to rotation of the earth on its axis at 15° per hour (Duffie and Bechman, 2013).

$$w = ST \times \frac{360}{24} \quad (3.3)$$

3.5.2.4 The azimuth angle (Φ): is the deviation of the normal to the surface from the local meridian. An object due north has an azimuth of 0^o, due east is 90^o , south and west is 180^o and 270^o respectively. For instance, at sunrise, the sun is positioned in the east at an azimuth of approximately 90^o, while at midday, it is located high in the sky at nearly 0^o azimuth (Ogbuisi, 2010).

$$\sin = \cos\delta\frac{\cos w}{\cos\beta} \quad (3.4)$$

Where:

θ_z= Zenith angle

δ= Declination angle

β = Tilt angle

ϕ = Azimuth angle

3.5.2.5 Zenith Angle (θ_z):is the angle between the vertical and the line to the sun, that is the angle of incident of beam radiation on a horizontal surface (Duffie and Beckman, 2013).

$$\theta z = cos^{-1}[coscos\delta cos\omega + sinsin\delta] \quad (3.5)$$

3.5.2.6 The optimum tilt angle for booster mirror

The optimum tilt angle for booster mirror (λ) is given by Sethi et al.(2013) as:

$$\lambda = \frac{90-2_z}{3} \quad (3.6)$$

3.5.2.7 Solar Radiation Theoritical Background

The radiation from the sun reaching the earth surface is comprised of beam and diffuse radiation. Diffuse radiation is due to the scattering of sunlight by the atmosphere, while beam radiation is the part that is not affected. The components of the beam form a larger part of the total radiation.

3.5.2.7.1 Incident radiation

To determine the incident beam radiation on a surface of arbitrary orientation, it is necessary to evaluated the geometrical ratio, R_b given by Duffie and Beckman (2013) as:

$$R_b = \frac{\cos\theta_i}{\cos\theta_z} \quad (3.7)$$

Where Θ_i is the angle of incidence of beam radiation relative to the normal of surface

Θ_z is the zenith angle of the sun

Where, the expressions $\cos\Theta_i$ and $\cos\Theta_z$ are evaluated as follows (Duffie and Beckman, 2013).

$$\text{Cos } \Theta_z = \cos \delta \sin \Theta + \cos\delta\cos Q\cos w \quad (3.8)$$

$$\text{Cos } \Theta_i = \cos\Theta_z \cos \beta + \sin \Theta_z \sin \beta \cos (\gamma_s - \gamma) \quad (3.9)$$

Where:

β = Tilt angle

γ_s= Surface azimuth angle

γ = Azimuth angle

δ = Declination angle

ϕ = Latitude of the location

W = Hour angle

The beam and diffuse radiation tilted surface are then given by Duffie and Beckman, (2013) as:

$$I_{bt} = I_b R_b \quad (3.10)$$

$$I_{dt} = I_d \frac{(1+\cos\beta)}{2} \quad (3.11)$$

Where:

I_{bt} = Beam radiation on a tilted surface (W/m^2)

I_{dt}= Diffuse radiation on a tilted surface (W/m^2)

I_b = Beam radiation on horizontal surface (W/m^2)

I_d = diffuse radiation on horizontal surface (W/m^2)

3.5.2.7.2 Reflection of radiation

When sun ray strikes a specula reflecting surface, the angle of incident is equal to the angle of reflection. Plane reflectors are used to increase the radiation flux amount onto the aperture of the coking chamber box. Reflectivity is the reflected energy to the incident energy.

The reflected radiation intensity is given by Duffie and Beckhman (2013) as:

$$I_r = \rho I_{bt} \tag{3.12}$$

Where:

I_r= Reflected radiation (W/m^2)

I_{bt} = Incident beam radiation on tilted surface (W/m^2)

$\rho$is the reflectivity

3.5.3 Energy analysis of solar cooker

3.5.3.1 Collector performance

In the evaluation of the collector performance, the following simplified energy balance equation can be used (Dasin, 2013):

$$Q_u = \left(F_{ta}\mathrm{I}_{av} - U_l(T_m - T_{am})\right)A_{sc} = M_w C_p(T_{bo} - T_{am}) \tag{3.13}$$

Where:

Q_u = Rate of useful heat energy extracted from the collector in (W)

F_{ta}= Product of the transmissivity of the glazing and the absorptivity of the absorber plate

I_{av}= Average solar radiation (W/m^2)

M_w= Mass flow rate (Kg)

U_l= Solar collector overall heat loss co-efficient in (W/m^{2}K)

T_{am}= Ambient temperature in (^{o}C)

T_m = Mean temperature (^{o}C)

T_{bo} = Boiling point of water temperature (^{o}C)

The mean temperature of air can be estimated through the relation (Hall, 1989)

$$T_m = \frac{T_{am}+T_{bo}}{2} \quad (3.14)$$

3.5.3.2 Collector Efficiency

Collector efficiency is defined as the ratio of the rate of useful thermal energy leaving the collector to the useable solar irradiance falling on the collector area (Fabio, 2008):

$$_c = \frac{Q_u}{A_{sc}I_{av}} \quad (3.15)$$

3.5.3.3 Thermal efficiency

The overall thermal efficiency of a solar cooker can be calculated from the following equation given by Elamin and Abdallah(2015) as:

$$_u = \frac{MwCw\Delta T_f}{I_{av}A_{sc}\ \Delta_t} \quad (3.16)$$

$_u$= Overall thermal efficiency

Mw = Mass of the water

ΔT_f= Difference between the maximum and ambient air temperature

I_{av}= Average solar intensity (w/m^2) during the time interval

A_{sc}= Surface collector area of the cooker

Δt = Time required to achieve the maximum temperature of the cooking vessel

3.5.4Collector Dimensions

3.5.4.1 Solar cooker surface collector area

The surface collector area A_{sc} of box solar cooker is from the following equation given by Ekechukwu and Abdussalam (2001) as:

$$A_{sc} = \frac{Mw\ C_p\ \Delta T}{I_{av}\ t} \quad (3.17)$$

Where:

M_w = Mass of water to be boiled

C_p = Specific heat capacity of water at constant pressure

ΔT = Change in temperature

I_{av} = Anticipated average total insolation (during the time, t)

η = Assumed overall cooker efficiency

t = Time desired for boiling of water in (sec)

3.5.4.2 Cooker wall insulation thickness

The insulation thickness, x of the solar cooker wall is given from Fourier's law of conduction given by Ekechukwu and Abdussalam(2001) as:

$$x = \frac{KA_{sc}\,\Delta Tp}{q_l} \tag{3.18}$$

Where

K is the thermal conductivity of the insulator (fibre glass)

ΔTp = change in temperature of absorber plate and that of ambient temperature

q_L = Desired maximum rate of heat loss through the cooker walls (q_L = 7% of incident average solar radiation) by Ekechukwu and Abdussalam(2001).

3.5.5 Stagnation temperature test.

Stagnation temperature test is an important parameter because it depicts the ability of a cooker develops and retains minimum temperature which in turn reflects on the quality of the design and performance. Therefore standardized stagnation temperature is given by Ashok and Sudhir(2009) as:

$$SST = 700\left(\frac{T_s - T_a}{I_{av}}\right) \tag{3.19}$$

Where:

SST = standard stagnation test

T_s= Maximum surface temperature

T_a= Ambient temperature

$$T_{st} = \left(\frac{700Mw}{\sigma}\right)^{1/4} \tag{3.20}$$

T_{st}= Theoretical maximum surface temperature (^{o}C)

M_w= is the mass of water in the cooking vessels (Kg)

σ = Stephen – Boltzman constant ($Wm^{-1}K^{-1}$)

3.5.6 Performance measures

The performance evaluation of the solar box cooker involves estimation of the following parameters: First figure of merit (F_1), Second figure of merit (F_2)

i. First figure of merit

The first figure of merit (F_1) of a solar box cooker is defined as the ratio of optical efficiency (ηo) and the overall heat loss coefficient (U_l). It is given as follows (Yusuf et al., 2014):

$$F_1 = \frac{T_{ps} - T_{am}}{I_{av}} \tag{3.21}$$

T_{ps}= stagnation plate temperature

T_{am}= average ambient tempt

I_{av}= average intensity of solar radiation

According to (Jagan and Madhu, 2007) for a good design solar box solar cooker, the first figure of merit ($F_{1)}$ should be at the range of 0.12 – 0.16

ii. Second figure of merit

The second figure of merit (F_2) is evaluated under full load condition and can be expressed by the expression given as follows (Yusuf et al., 2014):

$$F_2 = \frac{F_1(m_w c_w)}{A_{sc}} ln \left[\frac{1 - \frac{1}{F_1}\left(\frac{T_1 - T_{am}}{I_{av}}\right)}{1 - \frac{1}{F_1}\left(\frac{T_2 - T_a}{I_{av}}\right)} \right] \tag{3.22}$$

F_1 = first figure of merit (Km^2/w)

M_w = mass of water in kg

C_w = specific heat capacity (J/Kg^{o}C)

T_{am} = average ambient temperature

A_{sc} Surface collector area (m^2)

I_{av} Average solar radiation (W/m^2)

T_1 = initial temperature of water

T_2 = final temperature of water

According to (Jagan and Madhu, 2007) for a good design solar box cooker, the second figure of merit ($F_{2)}$ should be at the range of 0.254 – 0.490.

3.6 Design Calculations

Design Calculations for Solar Cooker.

Initial values	Formula/calculations	Result
Zaria location latitude is given as $\phi = 11°N$	**Optimum collector slope (β)** From equation (3.1), the optimum tilt angle β_{opt} is calculated as $\beta = \phi + 10°$ $\beta = 11° + 10° = 21°$	$\beta_{opt} = 21°$
n = 228 It is for the month of August with low solar radiation.	**The declination angle of sun (δ)** From equation (3.2), the declination angle for the 16th August, δ is $\delta = 23.45 sin\left(360 \frac{n + 284}{365}\right)$ $= 23.45 sin\left(360 \frac{228 + 284}{365}\right)$ $\delta = 13.45^{o}$	$\delta = 13.45^{o}$

ST=2:00	**Hour angle (w)** From equation (3.3), the hour angle w, at 14:00 hour solar time is calculated thus: $w = ST \times \frac{360}{24}$ $w = 2.00 \times \frac{360}{24} = 30°$	W = 30°
β = 21° δ = 13.45° w = 30°	**The azimuth angle ()** From the equation (3.4) the azimuth angle ϕ is given by $sin = \cos\delta \frac{\cos w}{\cos \beta}$ $sin = \cos(13.45) \frac{\cos 30}{\cos 21}$ $\sin = 0.9022$ $= sin^{-1}(0.922) = 64.44^{o}$	ϕ = 64.44°
δ = 13.45° w = 30° ϕ = 64.44°	**Zenith angle (Θ_z)** From equation (3.5) zenith angle Θ_z is given as $\Theta_z = \cos^{-1}(\cos\phi \cos\delta\cos w + \sin\phi \sin\delta)$ $\Theta_z = \cos^{-1}(\cos64.44\cos13.45\cos30 + \sin64.44\sin13.45)$ $= 55.02^{o}$	$\Theta_z = 55.02^{o}$

Θ_z = 55.02°	**The optimum tilt angle for booster mirror (λ)** From equation (3.6), the optimum tilt angle for booster mirror (λ) is given as $\lambda = \frac{90 - 2_z}{3}$ $\lambda = \frac{90 - 2(55.02)}{3}$ λ= -6.68^o	λ = -6.68^o
	Incident solar radiations. To determine the incident radiation on a surface of arbitrary orientation, , it is necessary to evaluated the geometrical ratio, R_b from equation (3.7) $R_b = \frac{\cos\theta_i}{\cos\theta_z}$ Also, from equation (3.8), making θ_i the subject, we get: $\theta_i = cos^{-1}[\cos\theta_z \, cos\beta + \sin\theta_z \, sin\beta cos(\lambda s - \lambda)]$	

	Where: $\lambda = \Phi - \lambda_s$ $\lambda_s = \Phi - \lambda$ $\lambda s = 64.44-(-6.68) = 71.12^o$	$\lambda_s = 71.12^o$
$\lambda_s = 71.12^o$ $\Phi = 64.44°$ $\lambda = -6.68^o$ $\theta_z = 55.02^o$ $\beta = 21^o$	From equation (3.9) $\theta_i = cos^{-1}[\cos\theta_z \cos\beta + \sin\theta_z \sin\beta \cos(\lambda s - \lambda)]$ $\theta_i = cos^{-1}[\cos 55.0 cos 21 + sin 55.02 sin 21 \cos(71.12 - (-6.68)]$ $= cos^{-1}(0.5972632)$ $\theta_i = 53.32^o$	$\theta_i = 53.32$
$\theta_i = 53.32^o$ $\theta_z = 55.02^o$	$R_b = \frac{\cos\theta_i}{\cos\theta_z}$ $R_b = \frac{\cos 53.32}{\cos 55.02}$ $R_b = 1.04 \approx 1$	$R_b = 1$

	The beam and diffuse radiations	
$R_b = 1$ $I_b = 795.5W/m^2$ (Akachukwu, 2011) for the month of August.	The beam and diffuse radiations on a titled surface is given in equation (3.10) and (3.11) The beam radiation on titled surface from equation (3.10) $I_{bt} = I_b R_b$ $I_{bt} = 795.5 \times 1$ $I_{bt} = 795.5W/m^2$	$I_{bt} = 795.5W/m^2$
$I_d = 683.5W/m^2$ (Akachukwu, 2011) for the month of August. β= 21°	The diffuse radiation on tilted surface is from equation (3.11) $I_{dt} = I_d\left(\frac{1+\cos\beta}{2}\right)$ $I_{dt} = 683.5\left(\frac{1+\cos 21}{2}\right)$ $I_{dt} = 660.8W/m^2$	$I_{dt} = 660.8W/m^2$

Reflectivity of transparent glass ρ = 1.5 I_{bt} = 795.5W/m^2	**Reflections of radiation** When sun ray strikes a specula reflecting surface, the angle of incident is equal to the angle of reflection (Ogbuisi, 2010). Plane reflectors are used to increase the radiation flux mount onto the aperture of the cooking chamber box. The reflected radiation intensity is given in equation (3.12) $I_r = \rho I_{bt}$ I_r = 1.5 x 795.5 I_r= 1193.25W/m^2	I_r= 1193.25W/m^2
	Energy analysis of solar cooker **Collector performance** In the evaluation of the collector performance, the energy equation is found from equation (3.13) $Q_u = \left(F_{ta}\mathrm{I}_{av} - U_l(T_m - T_{am})\right)A_{sc}$ Mean temperature (T_m) From equation (3.14) is given as:	

$T_{am} = 37^oC$ $T_{bo} = 100^oC$	$T_m = \frac{T_{am} + T_{bo}}{2} = \frac{37 + 100}{2} = 68.5^oC$	$T_m = 68.5^oC$
	$Q_u = \left(F_{ta}I_{av} - U_l(T_m - T_{am})\right)A_{sc}$ $= \left(0.88 \times 795.5 - 5(68.5 - 37)\right)0.56$ $Q_u = 303.8J$	$Q_u = 303.8J$
	Collector Efficiency Collector efficiency is found from equation (3.15) $_c = \frac{Q_u}{A_{sc}I_{av}}$ $_c = \frac{303.8}{0.56 \times 795.5} = 68.2\%$	$_c = 68.2\%$
$A_{sc} = 0.56m^2$ $M_w = 1.6kg$ $\Delta T_f = 10^oC$ $C_w = 4186kg^{-1}{}^oC^{-1}$ $I_{av} = 795.5\ w/m^2$ $\Delta t = 600sec$	**Thermal efficiency** From equation (3.16), the overall thermal efficiency is given as $_u = \frac{M_w C_w \Delta T_f}{I_{av} A_{sc} \Delta t}$ $u = \frac{1.6 \times 4186 \times 10}{795.5 \times 0.56 \times 600}$ $_u = 25\%$	$_u = 25\%$

Mw = 1.6kg ($0.0016m^3$) Cp = 4186J/kg/k ΔT = 110°C I_{av}= 795.5W/m^2(Akachukwu, 2011) t = 600sec (10 minute) $_c$= 0.682 Assuming collector breadth b = 0.7m A_{sc} = 1.5m^2	**Collector Dimension** **Solar cooker surface collector area** The surface collector area of the solar cooker is given from equation (3.17) $A_{sc} = \frac{MwC_p\Delta T}{I_{av}\, t\ _c}$ $= \frac{1.6\times4186\times(100-28)}{795.5\times600\times0.682}$ =1.4814m^2 = 1.5m^2 For the solar cooker length dimension A_{sc} = L × b L = $\frac{A_{sc}}{b} = \frac{1.5}{0.7}$ = = 2.1428m = 2m From the calculated length of collector, length of 2m is obtained. 0.8m is chosen in order to simplify the construction and to reduce the overall cost of production. This implies that collector area is 0.56m^2	A_{sc} = 1.5m^2 L =2m L = 0.8m

K= 0.04 W/m/k A_{sc} = 0.56 m^2 ΔTp = 110^{o}C q_L= 55.68 Desired maximum rate of heat loss through the cooker walls of incident average solar radiation (q_L = 7%) by (Ekechukwu and Abdussalam, 2001).	**Cooker insulation thickness** The insulation thickness, x of the wall solar cooker is given from fourier's law of conduction equation (3.18) $x = \frac{KA_{sc}\,\Delta Tp}{q_L}$ $= \frac{0.04 \times 0.56 \times 110}{55.68}$ = 0.0442m	x = 0.0442m
T_s = 107°C T_a = 37°C I_{av} = 795.5W/m^2	**Stagnation temperature test** The standardized stagnation temperature is given from equation (3.19) $SST = 700\left(\frac{T_s - T_{am}}{I_{av}}\right)$ $= 795.5\left(\frac{141-37}{795.5}\right)$ = 104^{o}C	SST = 104^{o}C

M_w = 1.6Kg $\sigma = 5.67 \times 10^{-8}$Wm^{-2}k^{-4}	Theoretical maximum surface temperature T_{st} is given from equation (3.20), $T_{st} = \left(\frac{700M_w}{\sigma}\right)^{\frac{1}{4}}$ $T_{st} = \left(\frac{700 \times 1.6}{5.67 \times 10^{-8}}\right)^{\frac{1}{4}}$ T_{st}=374.64°C	T_{st}=374.64°C
T_{ap} = 130º T_{am} = 30ºC (Ekechukwu and Abdussalam, 2001). I_{av} = 795.5w/m^2	**Performance measures** **i. First figure of merit** The first figure of merit is given in equation (3.21) $F_1 = \frac{T_{ap} - T_{am}}{I_{av}}$ $F_1 = \frac{130 - 30}{795.5}$ = 0.1257 Since F_1=0.1257 According to (Jagan and Madhu, 2007) for a good design solar box cooker, the first figure of merit ($F_{1)}$ should be at the range of 0.12 – 0.16	$F_1 = 0.1257$

F_1=0.1257 M_w = 1.6kg C_w = 4186J/kgk A_{sc} = 0.54m^2 T_1 = 37^{o}C T_2 = 100^{o}C I_{av} = 795.5W/m^2 T_{am} = 30^{o}C Δt = 1hr Δt = 3600sec	**ii. Second figure of merit** The second figure of merit is given in equation (3.22) $$F_2 = \frac{F_1(m_w c_w)}{A_{sc}\Delta_t} ln\left[\frac{1-\frac{1}{F_1}\left(\frac{T_1-T_{am}}{I_{av}}\right)}{1-\frac{1}{F_1}\left(\frac{T_2-T_{am}}{I_{av}}\right)}\right]$$ $$= \frac{0.1257 \times 1.6 \times 4186}{0.54 \times 3600} ln\left[\frac{1-\frac{1}{0.1382}\left(\frac{37-30}{795.5}\right)}{1-\frac{1}{0.1382}\left(\frac{100-30}{795.5}\right)}\right]$$ $$= \frac{841.8883}{2016} ln\left[\frac{0.936327}{0.36327}\right]$$ F_2 = 0.395 Also SinceF_2 = 0.395 According to Jagan and Madhu, (2007) for a good design solar box cooker, the second figure of merit (F_2) should be at the range of 0.254 – 0.490. It shows that both F_1 and F_2 values are within the range which indicates a good performance measurement.	F_2 = 0.395

3.7 The Design of Reflectors

Design Considerations:

i. The reflectors are specula with reflectivity $\rho_r = 0.8$

ii. The transmittance-absorptance products are function of angle of incidence.

iii. Shading by the collector and reflector on each other is neglected.

iv. Addition of reflector does not affect the shape factor.

Energy increased by the third reflector is given by (Rakesh*et al.,* 1994).

$$Q = (1 - S_{rc})\{(\alpha\tau)_{bt} I_{bt} + (\alpha\tau)_{dt} I_{dt} + \rho_r[(\alpha\tau)_{rt3} I_{r3} f_{ta} cos\theta_i]\} \quad (3.23)$$

Where:

S_{rc} = Shading factor on the collector due to the third reflector

$\alpha\tau$ = Transmittance-absorptance product

$$\alpha\tau = 1.03 - \frac{0.11}{cos\theta_i} \quad (3.24)$$

Where: $\theta_i = 53.32^o$ from the design calculation

Therefore $\alpha\tau = 0.845$

From the design consideration, $S_{rc} = 0$, $\rho_r = 0.8$

And from the design calculation table, $I_{bt} = 795.5$ W/m^2, $I_{dt} = 660.8$W/m^2, $I_{r3} = I_r = 1193.25$W/m^2, $f_{ta} = 0.88$and $\theta_i = 53.32^o$. $\alpha\tau = (\alpha\tau)_{bt} = (\alpha\tau)_{dt} = (\alpha\tau)_{rt3} = 0.845$

By computing the above parameters in equation 3.23, we get the energy gain due to third reflector.

$$Q = (1-0)\{0.845 \times 795.5 + 0.845 \times 660.8 + 0.8[0.845 \times 1193.25 \times 0.88cos53.32]\}$$

$$Q = 1654.6 \text{ J}$$

The total energy, $Q_T = Q + Q_u$

Where $Q_u = 303.8W$from design calculations

$$Q_T = 1654.6 + 303.8 = 1958.4 \text{ J}$$

The percentage energy increment due to third reflector is

$$\frac{Q}{Q_T} \times 100\% = \frac{1654.6}{1958.4} \times 100\% = 84.5\%$$

The reflectors are more effective when the solar incidence angle increases with the position of the sun and becomes less effective when the incidence angle on the reflector surface decreases. The expressions for the angles of incidence on the collector for the reflected rays are (Rakesh*et al.*, 1994).

$$cos\theta_{rc1} = -u_1 sin\beta_c cos\gamma_s - v_1 sin\beta_c cos\gamma_s - w_1 cos\beta_c \qquad (3.25)$$

$$cos\theta_{rc2} = -u_2 sin\beta_c cos\gamma_s - v_2 sin\beta_c cos\gamma_s - w_2 cos\beta_c \quad (3.26)$$

$$cos\theta_{rc3} = -u_3 sin\beta_c cos\gamma_s - v_3 sin\beta_c cos\gamma_s - w_3 cos\beta_c \quad (3.27)$$

Where:

The unit vectors in the directions of the reflected rays from the reflectors are respectively, $\bar{n}_{rc1}$, $\bar{n}_{rc2}$, $\bar{n}_{rc3}$, and may be expressed as (Rakesh*et al.*, 1994).

$$\bar{n}_{rc1} = u_1\bar{\imath} + v_1\bar{\jmath} + w_1\bar{k} \quad (3.28)$$

$$\bar{n}_{rc2} = u_2\bar{\imath} + v_2\bar{\jmath} + w_2\bar{k} \quad (3.29)$$

$$\bar{n}_{rc3} = u_3\bar{\imath} + v_3\bar{\jmath} + w_3\bar{k} \quad (3.30)$$

Where:

$$u_1 = -sin\theta_z cos\gamma + 2cos\theta_{r1} sin\beta_{r1} cos\gamma_s \quad (3.31)$$

$$u_2 = -sin\theta_z cos\gamma - 2cos\theta_{r2} sin\beta_{r2} cos\gamma_s \quad (3.32)$$

$$u_3 = -sin\theta_z cos\gamma - 2cos\theta_{r3} sin\beta_{r3} cos\gamma_s$$

For reflector 3, the tilt angle $\beta_{r3} = 90^0$since it is fixed. It implies that $sin\beta_{r3} = 1$

$$u_3 = -sin\theta_z cos\gamma - 2cos\theta_{r3} cos\gamma_s \quad (3.33)$$

$$v_1 = -sin\theta_z sin\gamma + 2cos\theta_{r1} sin\beta_{r1} sin\gamma_s \quad (3.34) \qquad v_2 = -sin\theta_z sin\gamma - 2cos\theta_{r2} sin\beta_{r2} sin\gamma_s \quad (3.35)$$

$$v_3 = -sin\theta_z sin\gamma - 2cos\theta_{r3} sin\gamma_s \quad (3.36) w_1 = -cos\theta_z + 2cos\theta_{r1} cos\beta_{r1} \quad (3.37)$$

$$w_2 = -cos\theta_z + 2cos\theta_{r2} cos\beta_{r2} \quad (3.38)$$

$$w_3 = -cos\theta_z + 2cos\theta_{r3}cos\beta_{r3}$$

For the third reflector $\beta_{r3} = 90^0$

$$w_3 = -cos\theta_z \qquad (3.39)$$

Where:

$\beta_{r1}$is the tilt angle of reflector R1.

$\beta_{r2}$is the tilt angle of reflector R2.

$\beta_{r3}$is the tilt angle of reflector R3.

$\beta_c$is the collector tilt angle.

$\theta_{r1}$is the angle of incidence of solar radiation on R1.

$\theta_{r2}$is the angle of incidence of solar radiation on R2.

$\theta_{r3}$is the angle of incidence of solar radiation on R3.

3.8 Solar Cooker Construction

The construction of solar cooker was carried out in Mechanical Engineering Department workshop of Ahmadu Bello University Zaria. The processess and methods of construction are presented in table 3.2 below:

Table 3.2: Construction Process for Solar Cooker

S/N	Component	Material	Process description	Equipment used
1	Absorber plate	Aluminium plate 2500mm	Cut two pieces of 810mm x 560mm from a	• Work Bench • Tape Rule

		x 1250mm x 3mm thick, Top bond glue, Matte black paint and Nails.	sheet of aluminuim plate of 2500mm x 1250mm x 3mm thick. Cut to form an angle of 21°. 1 piece of 806mm x 610mm cut from 2500mm x 1250 x 3mm thick to form the absorber plate base. 1 piece of 610mm x 560mm cut from 2500mm x 1250mm x 3mm to form the absorber plate upper side and 1 piece of 610mm x 250mm cut to form lower side from 2500mm x 1250mm x 3mm thick absorber plate. Abro silicon was used at four sides of the absorber plate to minimize heat loss. Nails were used to fix the absorber on the inner casing to form a cooking chamber. Matte	• Pencil • Straight Edge • Jig Saw • Screw Driver • Plier • Mallet • Hammer • Hack Saw

			black color was used to paint the inner cooking chamber for better heat conduction.	
2	Inner casing	Plywood 2244mm x 1122mm x 18mm timber	Cut two pieces of 830mm x 575mm from a sheet of 2240mm x 1122mm x 18mm plywood to form an angle of 21°. 1 piece of 830mm x 610mm cut from 2244mm x 1122mm x 18mm to form a base of the inner casing. 1 piece of 830mm x 610mm cut to form a sheet of plywood of 2244mm x 1122mm x 18mm to form a back view of the inner casing. 1 piece of 630mm x 255mm cut from 2244mm x 1122mm x 18mm plywood to form the front view of the	• Hammer • Work bench • Tape rule • Pencil • Straight edge • Panel saw • Jig saw • Jack plane • Screw driver • Pinchers • Plier • Mallet • Chisel • Hack saw

			inner casing. Nails were used to join each side of the inner casing. Nails were used to join each side of the inner casing. Araldite was used in all the four corners of the inner casing to minimize heat loss.	
3	Air gap	Six rolls of polystyrene (fibre glass)	The fiber glass was used as an insulating material in the air gap in between the inner and the outer casing to minimize heat loss.	• Pair of scissors
4	• Outer casing	Plywood 2244mm x 1122mm x 18mm timber	Cut two pieces of 900mm x 600mm from a plywood sheet of 2244mm x 1122mm x 18mm to form angle of 21°. Cut 1 piece of 880mm x 680mm from 2244mm x 1122mm x18mm to form the base	• Hammer • Work Bench • Tape Rule • Pencil • Straight Edge • Panel Saw • Jig Saw

			of the outer casing. Cut 700mm x 640mm and 700mm x 255mm from 2244mm x 1122mm x 18mm plywood to form back and front view of the outer casing respectively. Use nail to joint all the parts. Araldite at the jointed part to minimize heat loss.	• Jack Plane • Screw Drivers • Pinchers • Plier • Mallet • Chisel • Hack Saw
5	Reflector	Back silvered low reflectance glass (plane mirror) of 2244mm x 1122mm x4mm thick	Cut 1 piece of 900mm x 700mm from 2244mm x 1122mm x4mm plane mirror. Cut two pieces of 700mm x 345mm from 2244mm x 1122mm x 4mm sheet of plane mirror. Top bond glue to hold the reflectors on plywood frame.	• Tape Rule • Straight Edge • Work Bench • Pencil • Square Rule • Measuring tape • Pinchers

6	Glazing	Transparent glass of 2244mm x 1122mm x 4mm thick	Cut two pieces of 900mm x 700mm from 2244mm x 1122mm x 4mm transparent glass sheet.	• Tape rule • Straight edge • Work bench • Pinchers • Measuring tape • Square rule • Pencil
7	Reflector frame	2244mm x 1122mm x 18mm plywood sheet.	Cut two pieces of 700mm x 345mm from 2244mm x 1122mm x 18mm of the plywood sheet. Top bond glue to fix the reflectors in place.	• Hammer • Work Bench • Tape Rule • Pencil • Straight Edge • Panel Saw • Jig Saw • Jack Plane • Screw Driver • Pinchers • Plier • Mallet • Chisel

				• Hack Saw
8	Solar cooker system finishing	• Handle • Angle Bar • Hinges • Ash colour paint • Bolts and nuts screw • Polish • Abrasive • Flat Bar • Matte Black	Holes were drilled to fixed the handles in place for opening and closing of the reflector frames. Angle bar fixed with reflector frame to adjust its sliding such that surface azimuth angle. Polishing of the outer box solar cookers. Ash colour coated of the 0.020mm on the outside of the solar cooker. Matte black paint was coated of the 0.020mm inside the cooking chamber for heat retention.	• Generator air compressor • Air blower (electric) • Electric abrasive grander • Generator air • Compressor • scrapper

3.9 Cost of the Solar Cooker

The cost of materials, transportation and labour incurred in the fabrication of the solar cooker is presented in table 3.4 below:

Table 3.3: Costs analysis for the Solar Cooker

S/N	Materials	Quantity	Rate (N)	Amount (N)
1	Plywood sheet of 2244mm x1122 x18mm	3.5	9000	31,500
2	Thick timber wood cut of 50mm x 50mm x 3666mm	12 pieces	250	3000
3	Araldite	2	350	700
4	Matte black paint	2 liters	1350	2700
5	Flat bar	3	500	1500
6	Bolt and nuts screws	5	100	500
7	Screw nails	3 pieces	250	750
8	Ash colour paint	2 liters	1150	2300
9	Cellulose thinner	4 liters	3500	3500
10	Polish	2 liters	500	1000
11	Abrasive	3 pieces	200	600
12	Top Bond Glue	2	900	1800
13	3210mm x 2250mm x 4mm transparent glass	1	8000	8000
14	Polystyrene (fibre glass)	5 rolls	1000	5000
15	3210mm x 2250mm x 4mm back silvered low reflectance glass	1	8500	8500
16	Angle Bar Iron	3	370	1110
17	2 inch hinges	6 pairs	50	300
18	Handles	2 pairs	120	240

19	Prymer	1 litre	1500	1500
20	Masking tape	1	150	150
21	1 inch nail	1 Pound	200	200
22	1 ½ inch nail	1 pound	200	200
23	3 inch nail	2 pound	150	150
24	Fuel	3 liters	800	800
25	Transportation		5000	5000
	Total			**81,000**

3.10 Solar Cooker Model

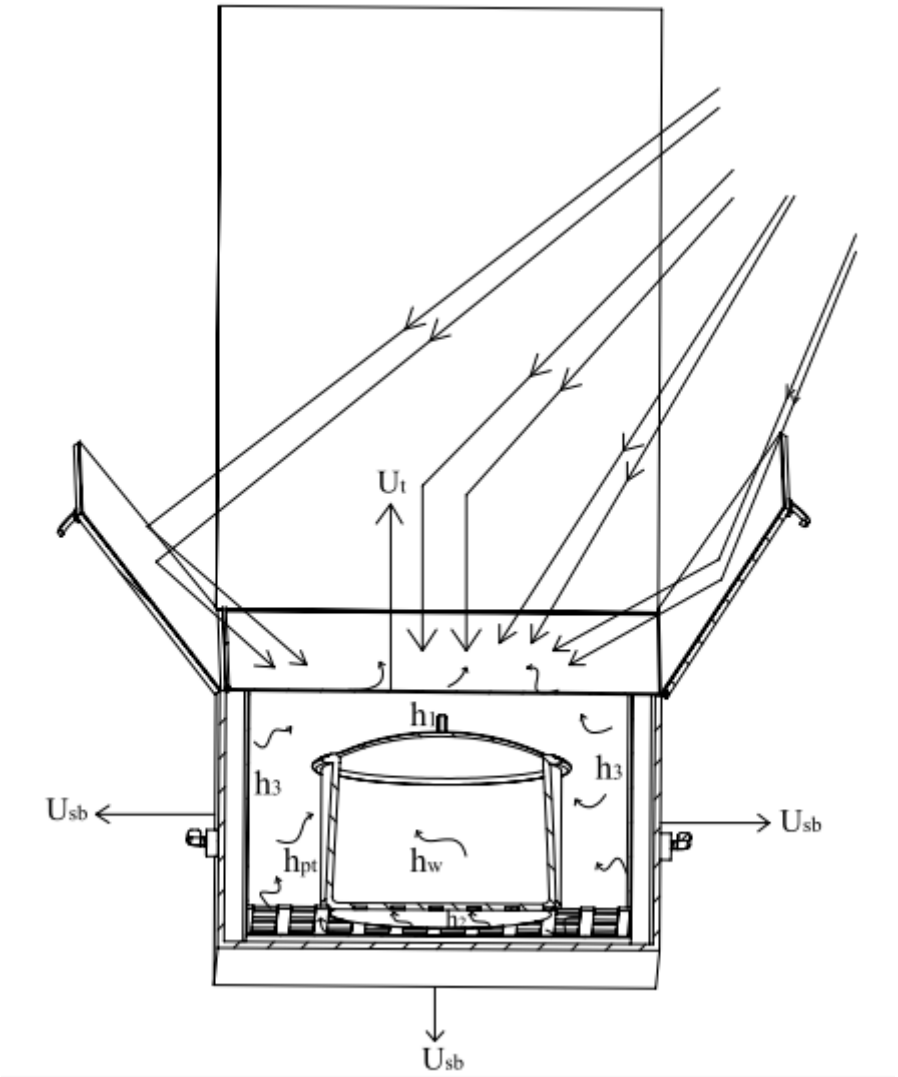


Figure 3.2: Modelling of Solar Cooking Chamber

The physical model postulated for the solar cooker is shown in Figure 3.2 above. The cooking chamber is heated by the radiation transmitted through the glazing. Heat is transferred from the side and bottom walls of the oven chamber at temperature, T_p, to the ambient air at T_{am}through the side and bottom loss coefficient U_{sb}, to the air in the oven chamber at temperature T_{io}, through the convection coefficients $h_2$and h_3, to glazing at temperature T_c, through the linear radiation heat transfer coefficient h_r. Heat is transferred to the cover glass from the air in the oven chamber through the heat transfer coefficient h_1, to the pot through the heat transfer coefficient h_{pt}, and finally to the water at temperature T_w,

through the heat transfer coefficient h_{wt}. Energy is lost from the glazing to the ambient air through the combined convection and radiation coefficient U_t.(Mohammed, 2015).

Energy balances carried out under steady state on the portion of glazing, cooking chamber, air in the cooking chamber, Absorber plate, pot and water yield the following equations (Mohammed, 2015):

Cooking chamber: $A_c Q_a + U_{sb} A_{sb}(T_a - T_p) + (A_c h_2 + (A_{sb} - A_c)h_3)(T_{io} - T_p) + h_r A_c(T_c -$

$Tp=0$ (3.23)

Absorber plate: $A_t h_t (T_{io} - T_t) + \frac{A_{pt} K_{pt}}{t_{pt}}(T_{pt} - T_t) = 0$ (3.24)

Portion of glazing: $U_t(T_a - T_c) + h_r(T_p - T_c) + h_1(T_{io} - T_c) = 0$ (3.25)

pot:$\frac{A_{pt} K_{pt}}{t_{pt}}(T_{pt} - T_t) + A_{spt}(T_{io} - T_{pt}) + A_{w-pt} h_{wt}(T_{wt} - T_{pt}) = 0$(3.26)

Air in the chamber: $h_1 A_c (T_c - T_{io}) + \{A_c h_c + (A_{sb} - A_c)h_3\}(T_p - T_{io}) = 0$ (3.27)

Water: $A_{w-pt} h_w (T_{pt} - T_{wt}) = q_u$ (3.28)

Where:

$h_w = 2.8 + 3V_w$ (3.29)

$U_t = h_w + h_{rca}$ (3.30)

$h_{rca} = {}_c\delta(T_c^2 + T_a^2)(T_c + T_a)$(3.31)

$h_1 = \frac{Nu_1 K_a}{a}$ (3.32)

$Nu_1 = 0.27 Ra_1^{\frac{1}{3}}$ (3.33)

$h_2 = \frac{Nu_2 K_a}{a}$ (3.34)

$Nu_2 = 0.27 Ra_2^{\frac{1}{3}}$ (3.35)

$$h_3 = \frac{Nu_1 K_a}{d} \quad (3.36)$$

For reflector: I_r is the beam insolation reflected on the plane reflector surface to the cooker glazing (Joshua, 2013):

For single reflector,

$$I_r = \rho_r I_{br} f_{rg} cos\theta_{rg} \quad (3.37)$$

Then for three reflectors,

$$I_r = 3\rho_r I_{br} f_{rg} cos\theta_{rg} \quad (3.38)$$

Where:

I_r= Beam insolation reflected on the plane reflector

ρ_r= Reflectivity of the plane mirror

I_{br}= Beam insolation incident on the plane reflector

f_{rg}= Reflector-glazing exchange factor.

If the reflector and the cooker are so adjusted that the cooker surface is completely exposed to the reflected radiation, then, $f_{rg} = 1$, and $\rho_r = 0.89$ (Joshua, 2013):

$$I_r = 3 \times 0.89 \times I_{br} \times 1 cos\theta_{rg}$$

$$I_r = 2.67 I_{br} cos\theta_{rg} \quad (3.39)$$

3.11 Simulation of Performance

Simulation models are developed in order to predict the performance of the box solar cookers. TRNSYS (Transient System Simulation) software and EES (Engineering Equation Solver) were used to model and simulate the operation of the system. TRNSYS consists of many subroutines that model subsystem components in any desired manner. Each component is represented as a box, which requires a number of constant parameters and time dependent outputs. A given output can however be used as an input to any number of other components. When a flow diagram is drawn in TRNSYS, a deck file is created containing information on all the components of the system, weather data file and the output format. TRNSYS also has

a provision for calling external programs like Microsoft excel, EES and so on (Mohammad, 2015).

3.12 Simulation of solar cooking chamber temperature

The solar cooker model was simulated using Zaria solar data for 28th, 30th and 31st October. The stagnation temperature of the cooker was simulated from 10:00am to 2:00pm on 28th October, while simulation with 1.6kg of water as load was carried out for 30th and 31st October. The solar collector design parameters such as tilt angle, collector depth, number of glazing, absorbtivityetc were inputted in the component of TRNSYS environment and output of water temperature and solar intensity were generated from 10:00am to 2:00pm

3.13 Modelling of Heat System

The heat system model consists of different components with inputs and outputs. The model shown in the TRNSYS simulation studio evaluates the average power absorbed by the solar oven within the time interval specified in the control cards. The model with the TRNSYS components and all interconnections are shown in Figure 3.3. The solar thermal system consists of weather data, reflectors and collector.

a. Weather data

   TRNSYS type109-tmy2 component was used to model the weather data. This component reads weather data at regular intervals from a data file, converts and processes the solar radiation data to obtain tilted surface radiation and other solar angle geometries for the collector surface.

b. Plane Reflectors

   For modelling the concentration of radiation by the reflectors, type 62 EXCEL components of TRNSYS was used. This TRNSYS type implements a link with Microsoft excel. The angle of incidence of the reflected radiation was evaluated using

the input values from TMY weather component. The output result was sent through the link to the equations component.

c. The collector

The modelling of collector as a macro consists of the equations components. The component calculates the transmissivities of the glazing for the incident and reflected radiation. Equation 3.15 was modelled in the equations component which calculates the solar energy absorbed per metre square of the collector. The parameters required for the model are given in Table 3.4. The periodic integrator component was used to calculate the integral of the energy absorbed in the collector within a specified period of time. A printer component was finally used to display the results at the end of each time interval.

Table 3.4: Simulation parameters for solar box cooker model

Parameter	**Value**
Number of glazing	2
Extinction coefficient of glazing	0.037
Refractive index	1.526
Absorbtivity	0.9
Reflectivity	0.9
Collector depth	0.4m

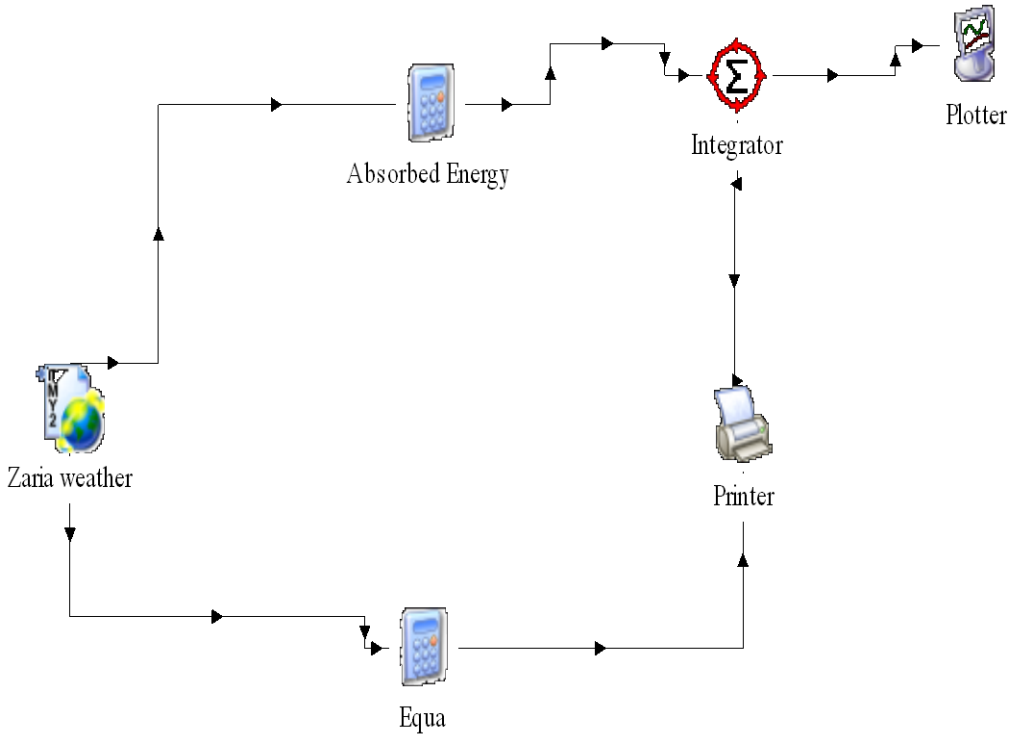


Figure 3.3: TRNSYS Simulation Model

3.14 Experimental Setup

The system was setup as shown in appendix A, were the solar cooker was facing north-south. One end of each of the three thermocouples was attached to the glazing, levelling tray and pot. A pyranometer was placed on the collector with its plane parallel to the plane of the collector. The small sized reflectors R1 and R2 were tilted at 45 and 15 respectively were the big sized reflector is fixed at 90^{o} using the optimum collector slope for Zaria location (21^{o}).

3.15 Test Procedure

The test was carried out on 28^{th} , 29^{th} , 30^{th} and 31^{st} October, 2017, at the Department of Mechanical Engineering workshop, Ahmadu Bello University, Zaria. The objective of the test was to obtain the continuous measurement of the system performance. In doing this, a consistent procedure was followed. Tests were conducted to determine the performance of the solar oven based on the ASAE S580 standard

The surface azimuth was adjusted every ten minutes to make up for the change in solar azimuth. Temperature and solar radiation were recorded every ten minutes as required. On the first day, the temperatures of the oven chamber, glazing and ambient air were recorded from 10:00am to 2:00pm with no load. On the second day, the system was setup with 1.6 kg of water in the pot. The pot was emptied and refilled when the temperature of water reaches 90□C.

3.16 Error Analysis

The root mean square Error (RMSE) was used to determine the level of deviation of the predicted result from the actual result. The RMSE measures the quality of fit between the actual data and the predicted model (Julien et al., 2013).

The RMSE of a model prediction with respect to the estimated variable X_{model} is defined as the square root of the mean squared error (Neil, 2010).

$$RMSE = \sqrt{\frac{\sum^{n}_{i=1}(X_{obsi} - X_{model,i})^2}{n}}$$

Where:

X_{obsi}= Observed values

$X_{model,i}$= Modelled values

The lower the mean Absolute Error or the Bias percentage value, the better the performance of the model (Neil, 2010).

Furthermore, the Nash-Sutcliffe Co-efficient of Efficiency (NSE) defined as follows (Neil, 2010).

$$NSE = 1 - \frac{\sum^{n}_{i=1}(X_{obs,i} - X_{model})^2}{\sum^{n}_{i=1}(X_{obs,i} - \overline{X_{obs}})^2}$$

Where:

X_{obsi} = Observed values

$X_{model,i}$= Modelled values

$\overline{X_{obs}}$= Mean observed value

NSE is generally used to quantitatively describe the accuracy of model outputs. Nash-Sutcliffe efficiencies can range from -∞ to 1. An efficiency of 1 (NSE = 1) corresponds to a perfect match between model and observations. An efficiency of 0 indicates that the model predictions are as accurate as the mean of the observed data, whereas an efficiency less than zero (-∞< E < 0) occurs when the observed mean is a better predictor than the model (Julien *et al.*, 2013).

CHAPTER FOUR

RESULTS AND DISCUSSION

4.1. The Variation of Solar Insolation with time

Figure 4.1 shows the average solar radiation incident on surfaces at different time intervals for the 4 conservative days. The fluctuations indicate the effects of cloud cover after each 10 minutes to know the average intensity of the sun from 10:00am to 2:00pm. The curve line is a regressional line showing line of best fit for the co-efficient of determination (r^2) which was found to be 91.87% .

This is the curve; it shows the graph for the four days along with the polynomial curve for the average of the four days

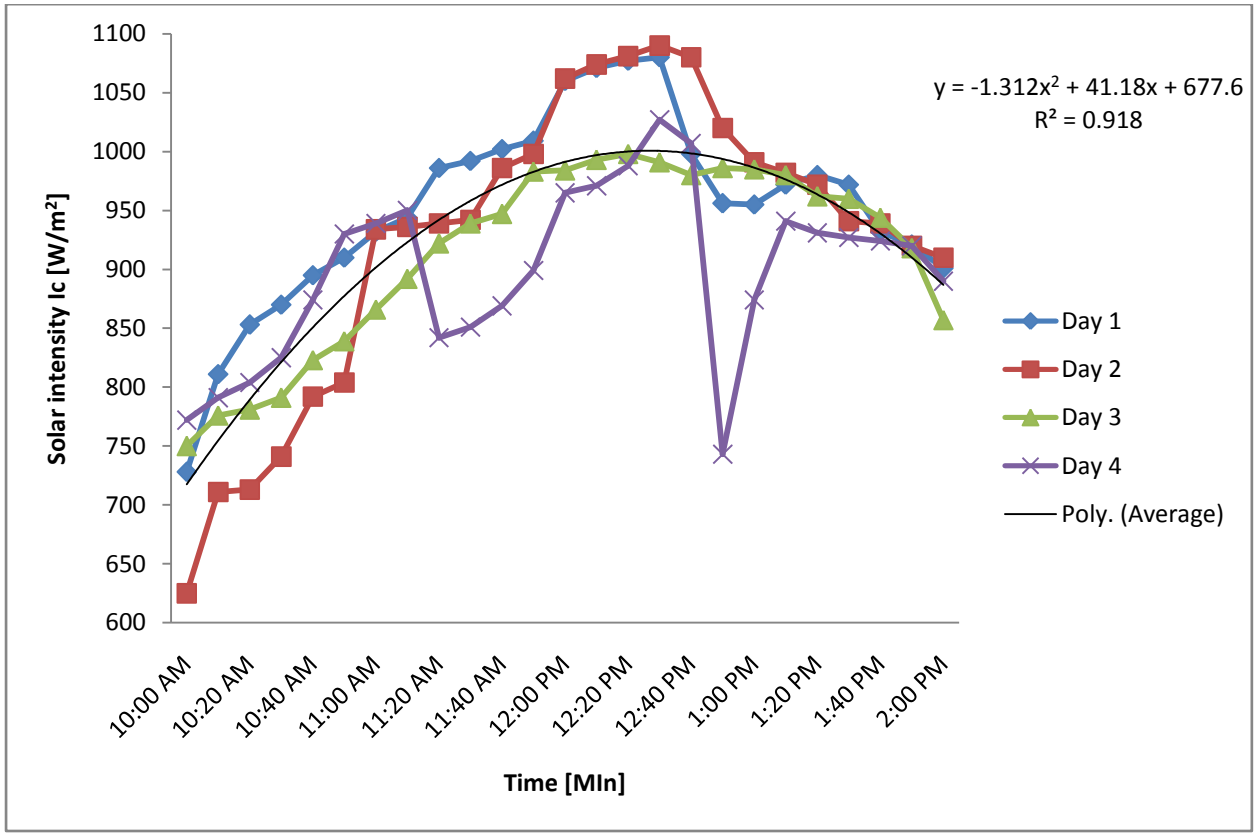


Figure 4.1: Variation of Average Solar Intensity with time from 28/10/2016 to 31/10/2016

4.2 Design month

Figure 4.2, shows solar radiation observer and presents the incident solar radiation on a horizontal surface and ambient temperature on 16th August (5448-5472hrs) in Zaria. It can be observed that there is steady increase in solar radiation intensity from 12 noon (5460hrs) until it reaches its peak at about 2 p.m. (5462hrs), from then it decreases gradually till 8p.m (5468hrs) when the sun sets. The solar oven model was simulated within this time interval (12noon-2:00p.m).

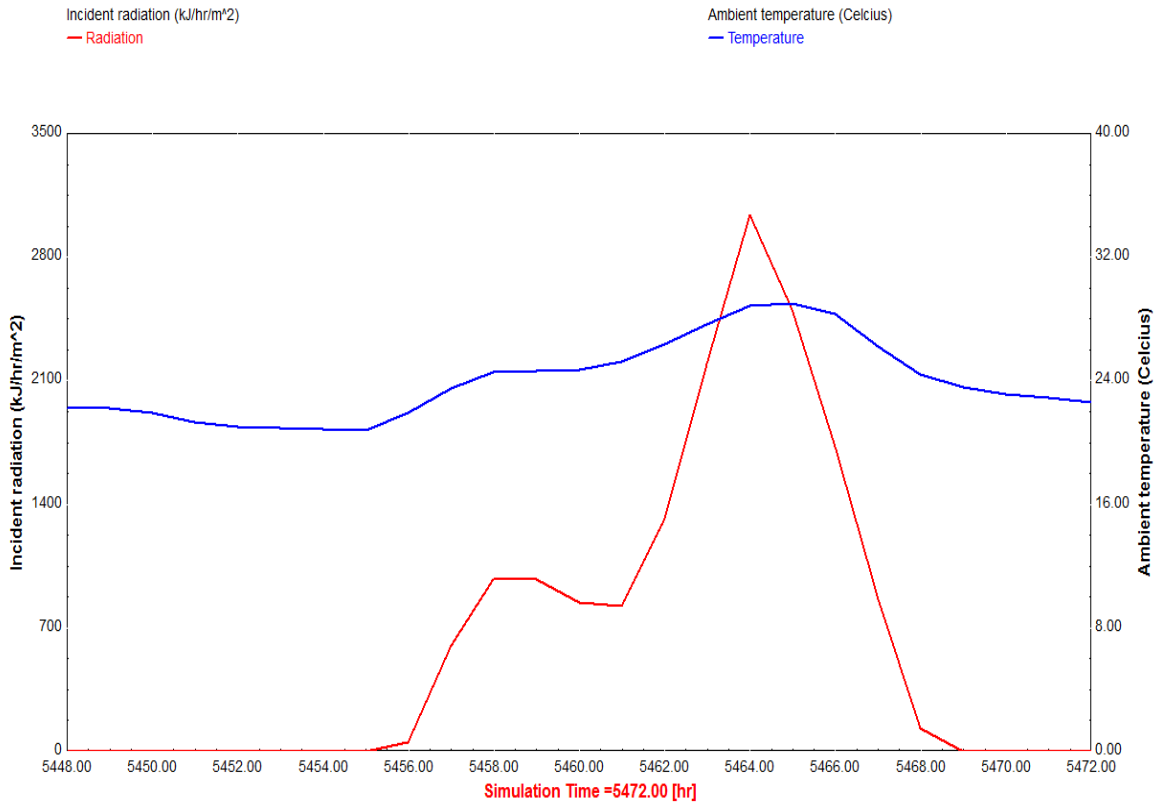


Figure 4.2: Solar radiation and ambient temperature variation for 16th August for Zaria.

Source: (Mohammed, 2015)

4.3 Variations of Simulated and experimental collector efficiency

Figure 4.3 shows the variation of simulated and experimental collector efficiency. From the figure, it was found that both the simulated and the experimental results follow the same

trends. And also using excels software, the co-efficient of determination (r^2) for both the simulated and experimental results were found to be 98.8% and 94.1% respectively.

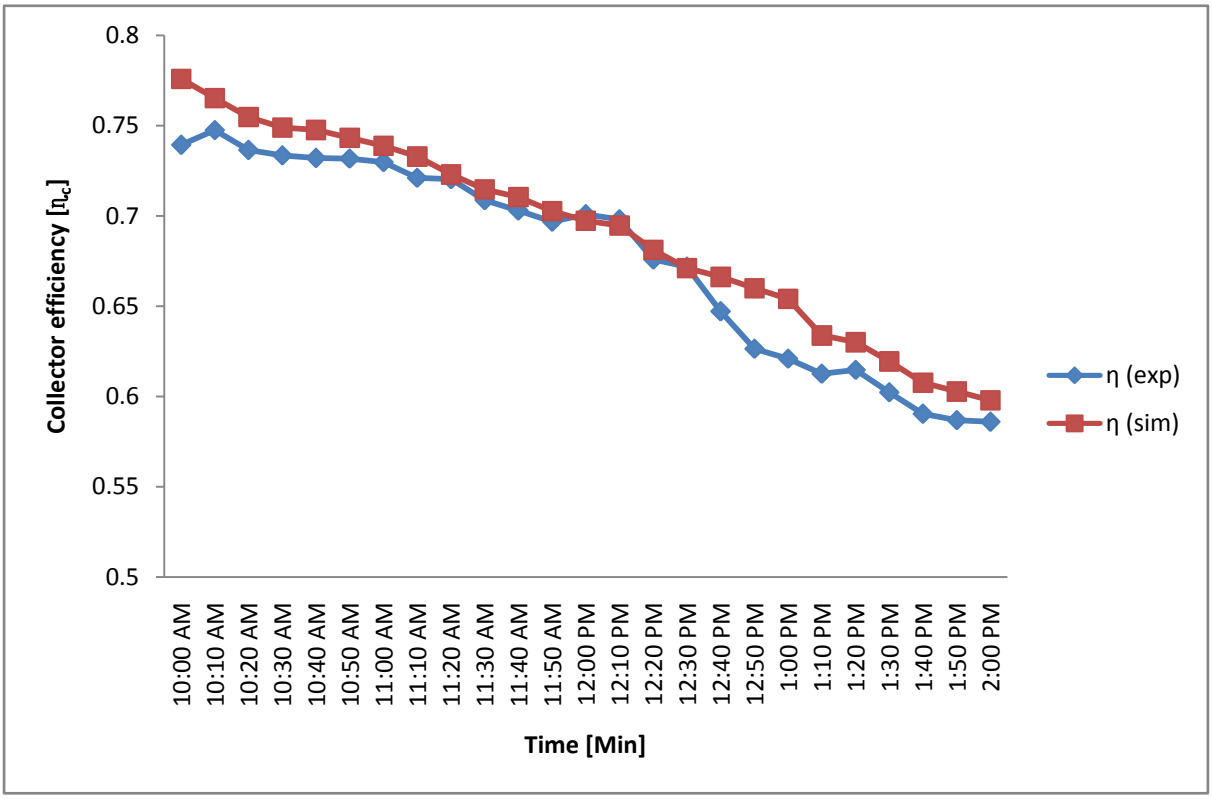


Figure 4.3: Variation of efficiency on the collector surface over time difference for simulation and experimental results.

4.4 Results Generated from TRNSYS and EES modelling

The results obtained from Transient System Simulation (TRNSYS) and the program written with the EES are shown in Appendix E

4.5 Comparison of simulated and experimental results

Figure 4.4 shows the variation of experimental and simulated results of solar radiations from 10am-2pm for 28th October, 2016. From the figure, the experimental solar radiation rises from 710 W/m^2 at around 10:10am gradually and reaches 11:10am. Were at 11:10am, there

was rapid increase due to the clarity of the sky which leads to high solar radiation. It reaches its peak value at 12:30pm. From then, the radiation was dropping up to 2pm. And from the figure below, both the simulation and the experimental value follows the same trend.

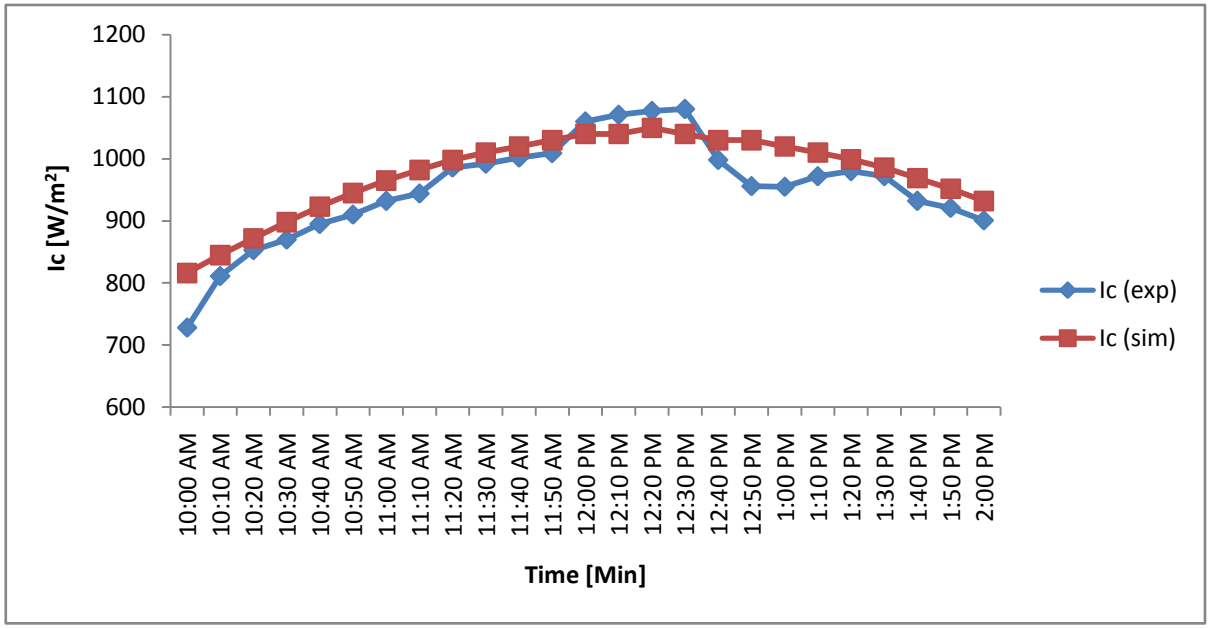


Figure 4.4: Experimental and simulated incident solar radiation with local time (28th October, 2016)

Figure 4.5 below is a graph of experimental and simulation stagnation temperature readings against time. From the figure 4.5, it can be seen that at 10:00am, the experimental stagnation temperature is around 64°C. Then at 10:10am that is after 10minutes, it increases to around 70°C. The increment in temperature was due the availability of the solar radiations during the day. Also, it can be seen that 10:20am, the stagnation temperature then increases to around 76°C. This shows that from 10:10am to 10:20am, the increase in stagnation temperature is 7°C. That was how the stagnation temperature increases continuously with time up to 1:00pm. At 1:00pm to 1:20pm the temperature was around 137°C the stagnation temperature was constant at this time interval due to the intermittent cloud cover. And there wasn't drop in temperature due to good insulation in the solar cooker. The Stagnation temperature was

around 143^{o}C at 1:30pm. Then after 10minutes, the stagnation temperature drops to around 138^{o}C due to low solar radiation at that moment.

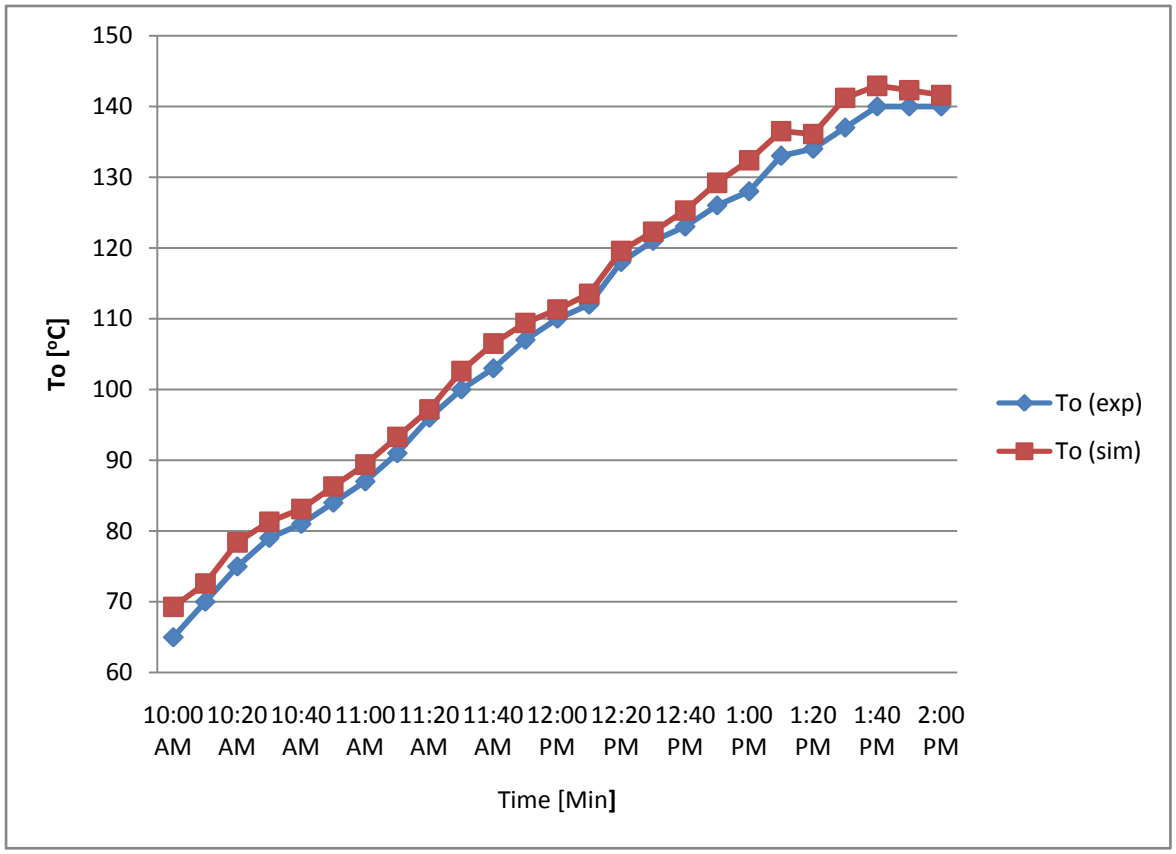


Figure 4.5: Experimental and simulated stagnation temperature with local time (28th October, 2016)

Figure 4.6 below is a graph of experimental and simulation results for ambient temperature for 28th October, 2016. From the figure, it can be seen that at 10:00am, the ambient temperature in the morning was around 28^{o}C. After 10minutes, that is at 10:10am, the ambient temperature increases to around 29^{o}C due to clarity of the sky. At 10:10am to 10:20am, the ambient temperature was constant due to the effect of cloud. Also, at 10:20am to10:30am, the ambient temperature increases to around 30^{o}C due to clarity of the sky. Then, from 10:30am to 10:40am, the ambient temperature was constant due to the intermittent

cloud cover. From 10:40am to 10:50am, the ambient temperature increased to around 32^{o}C. This was due to high solar intensity. The ambient temperature reaches its peak value at 11:30am to 12:10pm were the temperature was at 35^{o}C at higher solar radiation. Then from 12:10pm to 12:20pm, the ambient temperature drops to 31^{o}C due to the intermittent cloud cover. The temperature is also constant from 12:20pm to 12:30pm due to cloudy effect. All the fluctuations that occurred were due to cloudy effects. And the readings stops at 2:00pm were the ambient temperature is at 35^{o}C.

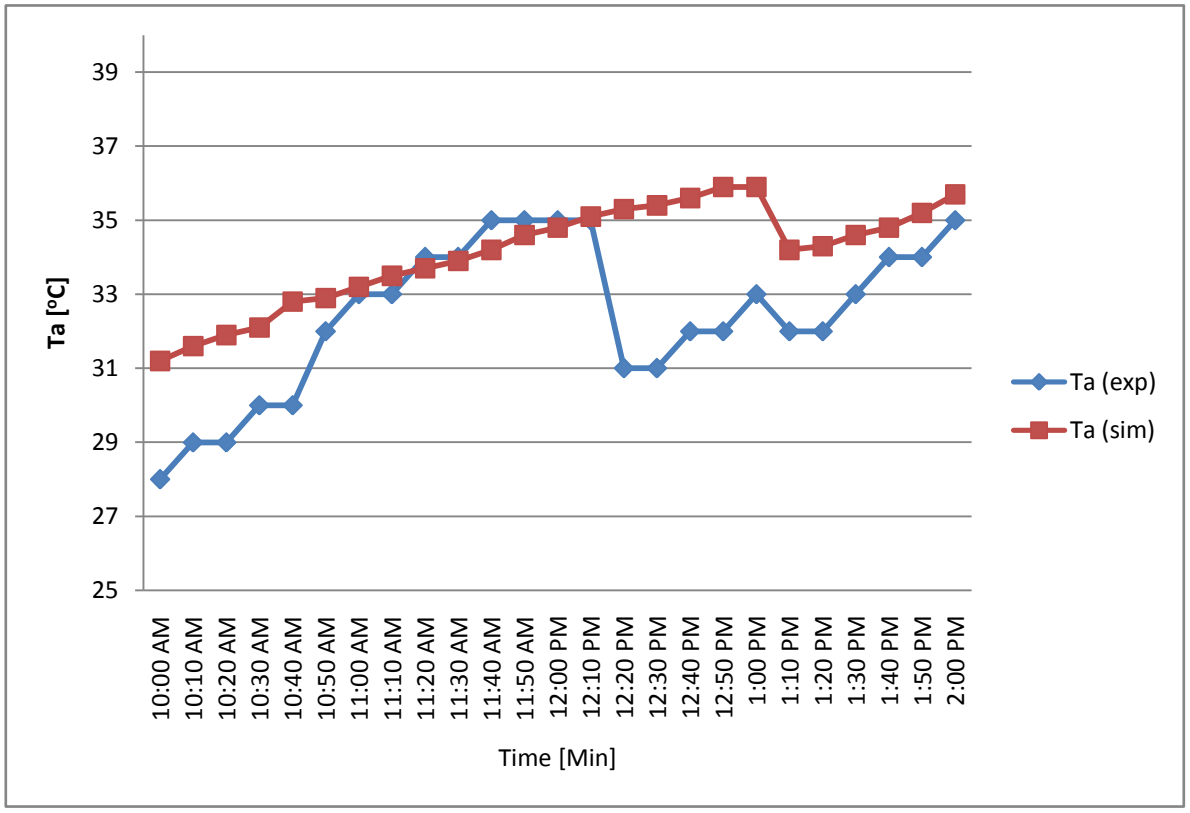


Figure 4.6: Experimental and simulated ambient temperature with local time (28th October, 2016)

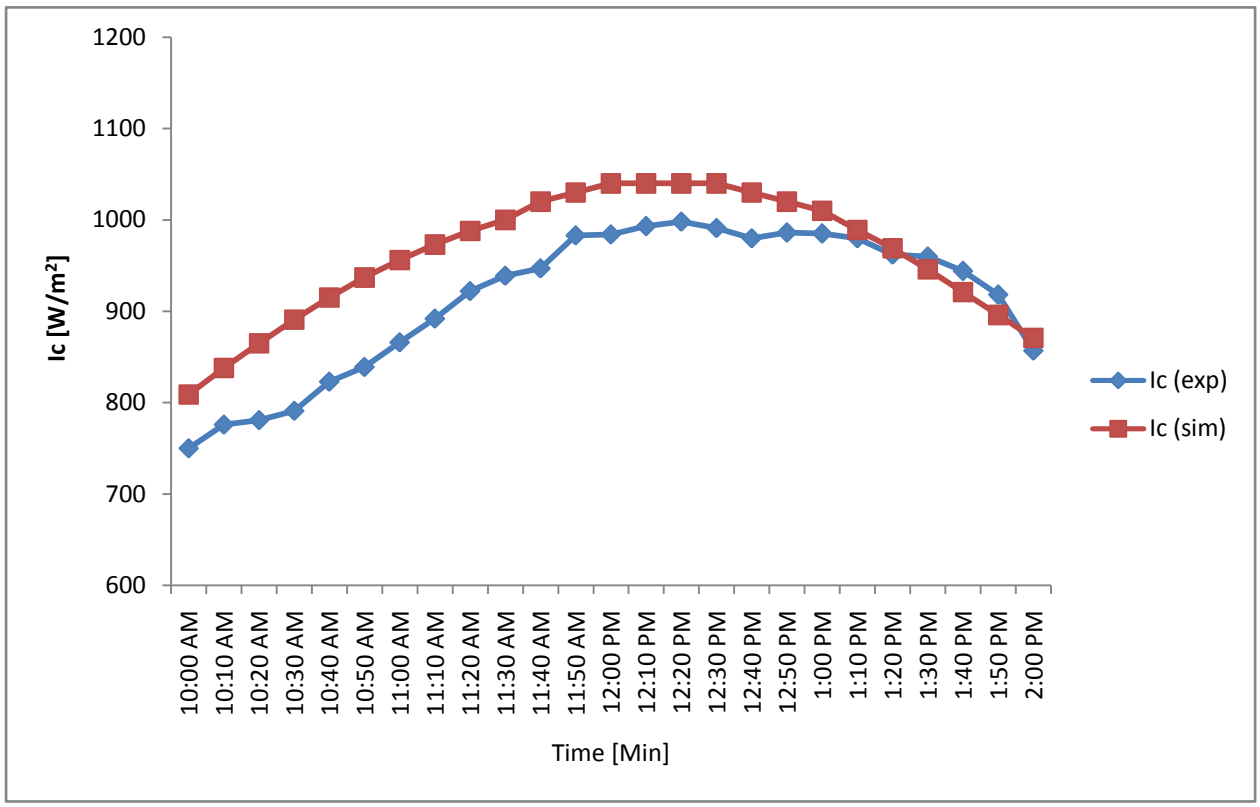


Figure 4.7: Experimental and simulated incident solar radiation with local time (30th October, 2016)

Figure 4.8 is the experimental and simulation water temperature with local time (30th October, 2016). As seen from the figure, the taking of the experimental readings starts at 10:00am were the water temperature is round 44°C. Then after 10 minutes, the temperature rises to around 48°C. This indicates that: there was an increment of 4°C within 10minute. This was due to the presence of solar radiation during the day. Then, at 10:10am to 10:20am, it can be seen that the temperature rises to around 57°C. It shows that at this time interval, the difference in water temperature is 9°C. The increase in the temperature of water by 9°C was due to the rise of solar radiations. At 10:20am to 10:30am, the water temperature rises from 57°C to around 69°C. It shows that at this interval of time, the increment of water temperature is 12°C. This was due to further increase in solar radiation. That was how the water temperature increase with time till 11:00am were the temperature is 87°C. At this time, the

water is then poured away and cold water was introduced into the pot and was transferred to the cooking chamber. The taking of the reading continued from 11:10am were the water temperature is around 51^{o}C. Then after 10minutes, the water temperature rises to around 57^{o}C. This indicates that the increment is 6^{o}C. And it shows that the solar radiation intensity drops compared to that from 11:20am to 11:30am were the increment was 12^{o}C. This occurred due to intermittent cloud cover in that interval of time. At 11:30am to 11:40am, the temperature increases from 57^{o}C to around 64^{o}C. The rise in temperature at this interval is 7^{o}C due to presence of solar radiation. From 11:40am to 11:50am, the increase in water temperature was from 64^{o}C to around 69^{o}C. The increment in water temperature is 5^{o}C in the presence of sunlight. Then from 11:50am to 12:00am, there was high increase in water temperature from 69^{o}C to around 88^{o}C within 10minutes interval. This occurred due to high solar radiation and clarity of the sky. At 12:00am, the water was poured away and cold water was introduced to the pot and transferred to the cooking chamber of the solar cooker were the taking of the readings continued after 10minutes. Then water temperature increased to around 53^{o}C. The taking of the reading continued after each interval of 10mintues till 1:00pm were the water temperature is around 87^{o}C. Then at 1:00pm, the hot water was poured away and cold water at room temperature was introduced to the cooking chamber, were after one hour the temperature reaches to 89^{o}C at round 2:00pm.

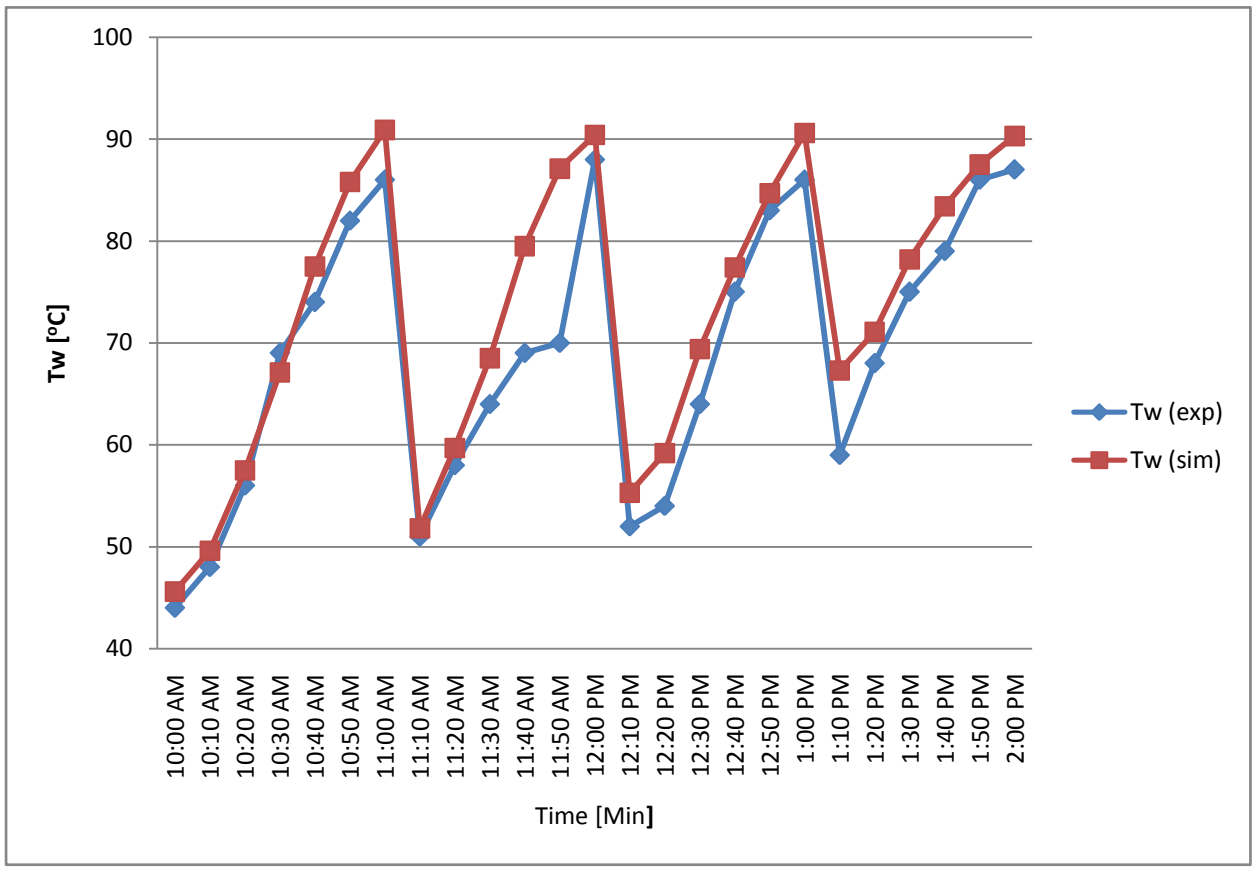


Figure 4.8: Experimental and simulation water temperature with local time (30th October, 2016)

Figure 4.9 below is the experimental and simulation ambient temperature with local time (30th October, 2016). From the figure, it can be seen that the experimental ambient temperature from 10:00am to 10:20am was constant were the temperature shows 28°C. That is to say: there wasn't change in ambient temperature for about 20minutes.This was due to intermittent cloudy cover. Then from 10:30am to 10:40am, the ambient temperature rises from 28°C to around 29°C due to high solar radiation. Then, from 10:30am to 10:40am, the ambient temperature was constant due to intermittent cloudy effect during the day. From 10:40am to 10:50am, the ambient temperature rises from 29°C to 30°C in the presence of solar radiation. That was how the ambient temperature keep on rising during the day and it reaches its peak value at around 1:40pm were the ambient temperature was found to be 35°C.

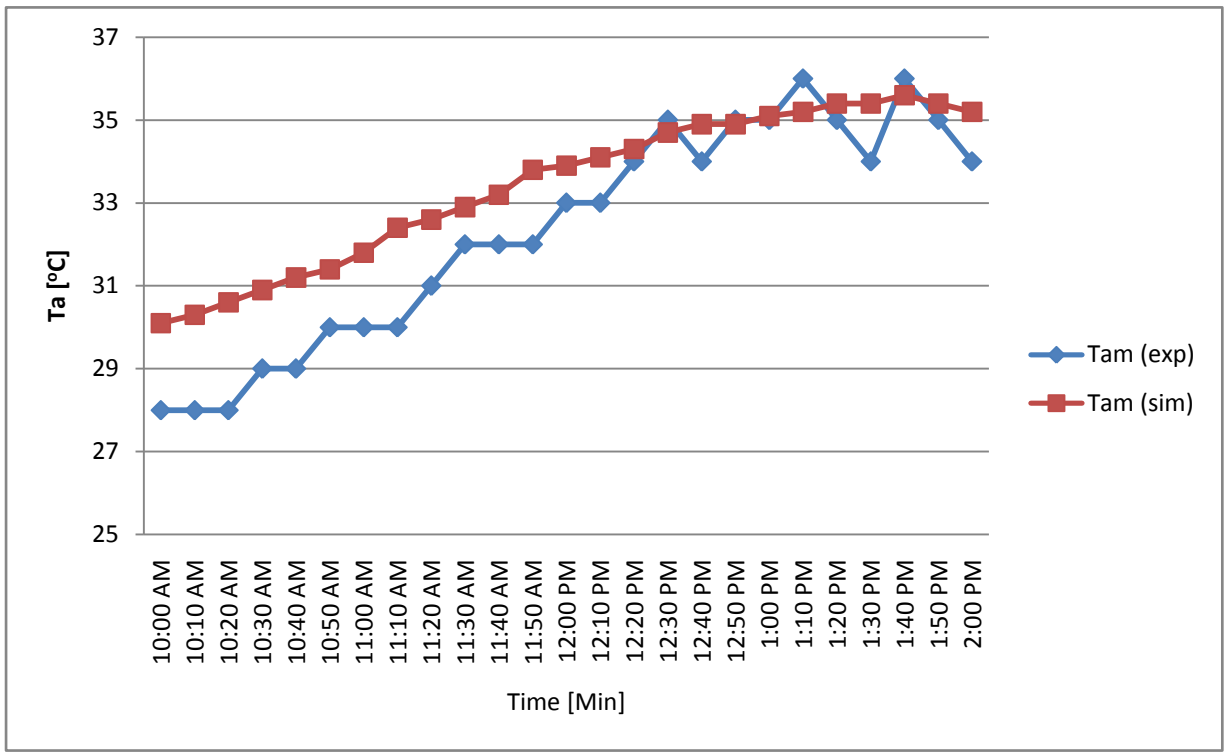


Figure 4.9: Experimental and simulation ambient temperature with local time (30th October, 2016)

Figure 4.10 shows the simulated and experimental solar radiation trends for 31st October, 2016. From the results, the simulated values rises constantly from 10:00am at around 800 W/m^2 and reaches its peak value at around 12:20pm were it starts dropping until 2pm. While for the experimental result, the value rises constantly from 770 W/m^2 at 10:00am to about 920 W/m^2 at 11:10am. Then it drops from 11:10am-11:20am due to the intermittent cloud cover. The radiation then rises from 11:20am and reaches its peak value at around 1020 W/m^2 at 12:30pm. From there, it falls rapidly from 12:30pm to 12:40pm due to the intermittent cloudy effects and then constantly from 12:40pm to 2:00pm in clear sky.

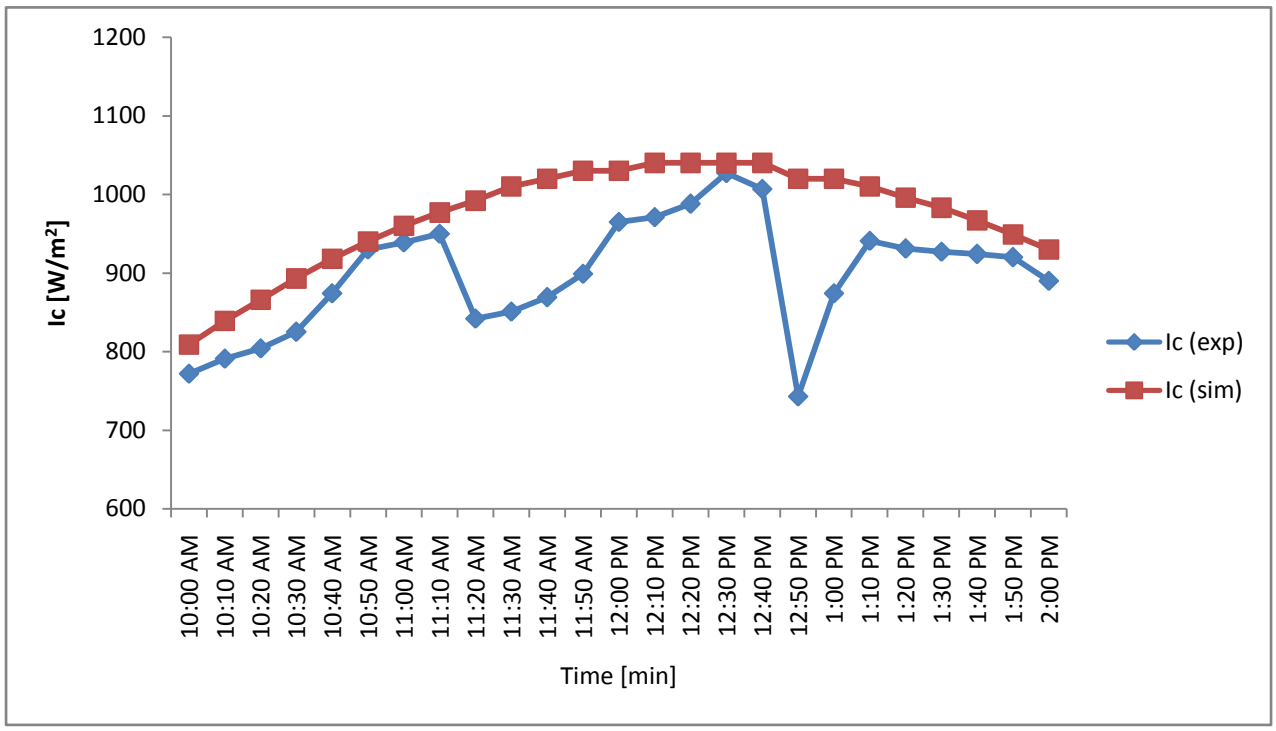


Figure 4.10: Experimental and simulated incident solar radiation with local time (31th October, 2016)

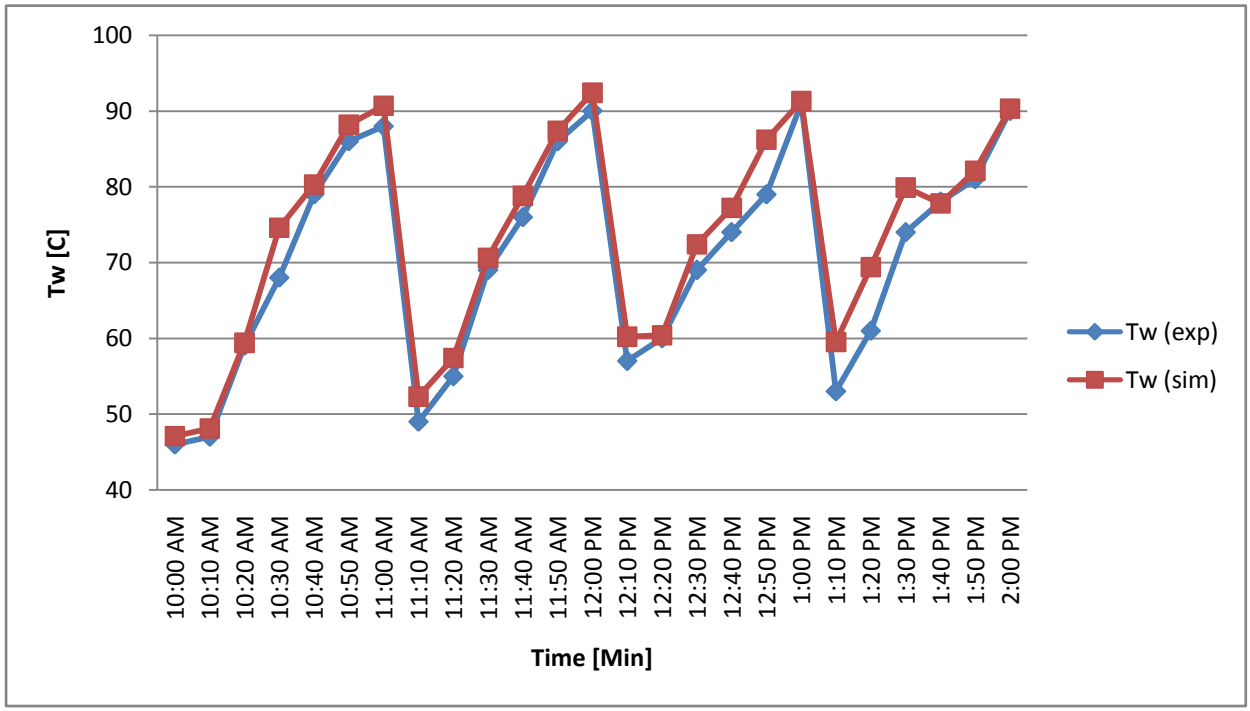


Figure 4.11: Experimental and simulated water temperature with local time (31th October, 2016)

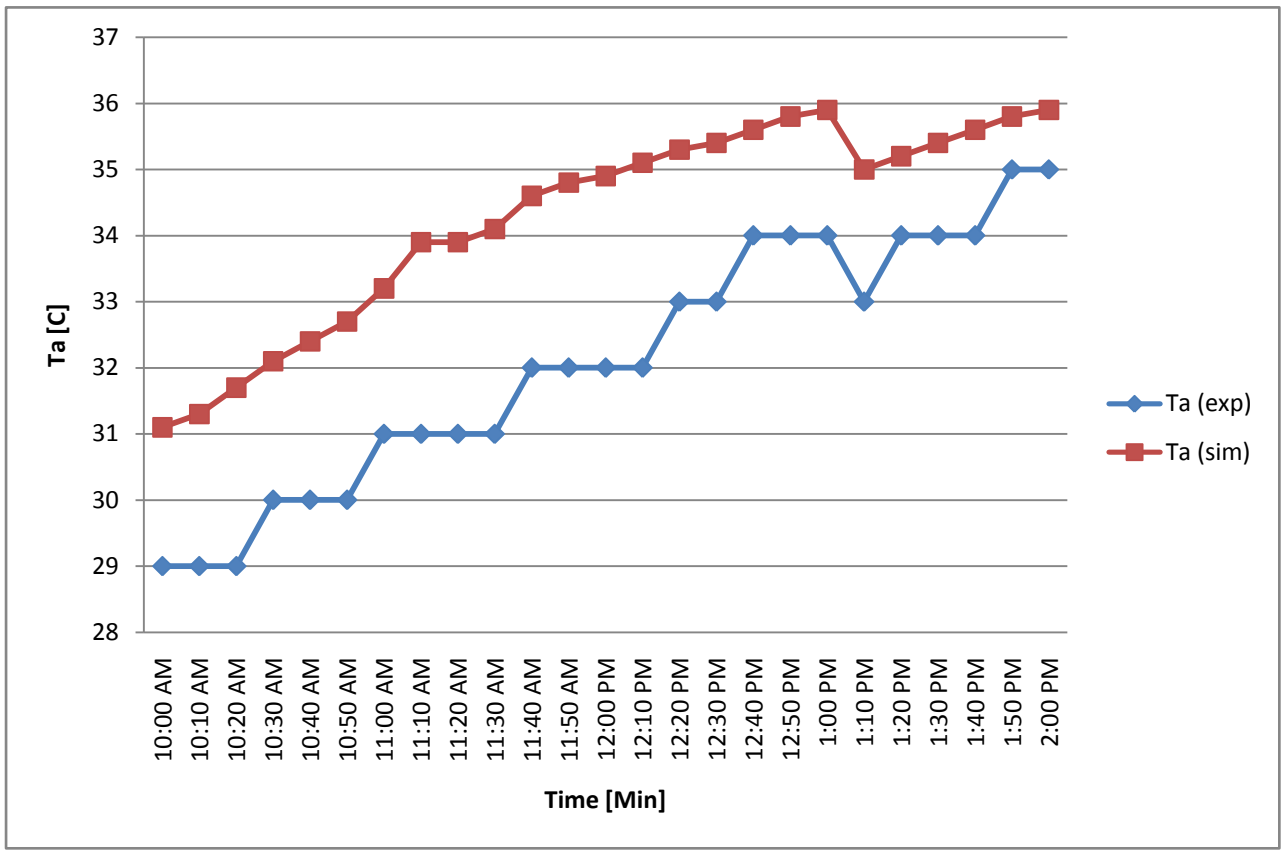


Figure 4.12: Experimental and simulated ambient temperature with local time (31th October, 2016)

4.6 Error Analysis of the comparison between experimental and simulation results

Analysis of error of the comparison between experimental and simulated result of 30th and 31st October are presented Table 4.8 below:

Table 4.1: simulated result with experimental result of 30th October, 2016 using RMSE and NSE

Time [min]	T_{Dexp}	T_{Dsim}	RMSE CALCULATION		
			$T_{Dsim} - T_{Dexp}$	$(T_{Dsim} - T_{Dexp})^2$	$(T_{Dsim} - \overline{T_{Dexp}})^2$
10:00AM	16	15.5	-0.5	0.25	451.9876
10:10AM	20	19.3	-0.7	0.49	372.49
10:20AM	28	26.9	-1.1	1.21	723.61
10:30AM	40	36.2	-3.8	14.44	1310.44
10:40AM	45	46.3	1.3	1.69	2143.69
10:50AM	52	54.4	2.4	5.76	2959.36
11:00AM	56	59.1	3.1	9.61	3492.81
11:10AM	21	19.4	-1.6	2.56	376.36
11:20AM	27	27.1	0.1	0.01	734.41
11:30AM	32	35.6	3.6	12.96	1267.36

11:40AM	37	46.3	9.3	86.49	2143.69
11:50AM	38	53.3	15.3	234.09	2840.89
12:00PM	55	56.5	1.5	2.25	3192.25
12:10PM	19	21.2	2.2	4.84	449.44
12:20PM	20	24.9	4.9	24.01	620.01
12:30PM	29	34.7	5.7	32.49	1204.09
12:40PM	41	42.5	1.5	2.25	1806.25
12:50PM	48	49.8	1.8	3.24	2480.04
1:00 PM	51	55.5	4.5	20.25	3080.25
1:10 PM	23	32.1	9.1	82.81	1030.41
1:20 PM	33	35.7	2.7	7.29	1274.49
1:30 PM	41	42.8	1.8	3.24	1831.84
1:40 PM	43	47.8	4.8	23.04	2284.84
1:50 PM	51	52.1	1.1	1.21	2714.41
2:00 PM	53	55.1	2.1	4.41	3036.01
TOTAL	919	990.1	71.1	580.89	43821.43

AVERAGE	36.76	39.604	2.844	23.2356	1752.857

$$RSME = \sqrt{\frac{\sum_{i=0}^{n}(T_{D\ sim} - T_{D\ exp})^2}{n}}$$

$$= \sqrt{\frac{580.89}{25}} = 4.8203℃$$

$$NSE = 1 - \frac{\sum_{i=0}^{n}(T_{D\ sim} - T_{D\ exp})^2}{\sum_{i=0}^{n}(T_{DSim} - \overline{T_{D\ exp}})2}$$

$$= 1 - \frac{580.89}{43896.48}$$

$$= 0.9867$$

Table 4.2: simulated result with experimental result for 31th October, 2016 using RMSE and NSE

Time [min]	T_{Dexp}	T_{Dsim}	RMSE CALCULATION		
			$T_{Dsim} - T_{Dexp}$	$(T_{Dsim} - T_{Dexp})^2$	$(T_{Dsim} - \overline{T_{Dexp}})^2$
10:00 AM	17	16	-1	1	507.1504
10:10 AM	18	16.8	-1.2	1.44	282.24
10:20 AM	30	27.7	-2.3	5.29	767.29

10:30 AM	38	42.5	4.5	20.25	1806.25
10:40 AM	49	47.9	-1.1	1.21	2294.41
10:50 AM	56	55.5	-0.5	0.25	3080.25
11:00 AM	57	57.5	0.5	0.25	3306.25
11:10 AM	18	18.4	0.4	0.16	338.56
11:20 AM	24	23.5	-0.5	0.25	552.25
11:30 AM	38	36.5	-1.5	2.25	1332.25
11:40 AM	44	44.2	0.2	0.04	1953.64
11:50 AM	54	52.6	-1.4	1.96	2766.76
12:00 PM	58	57.5	-0.5	0.25	3306.25
12:10 PM	25	25.1	0.1	0.01	630.01
12:20 PM	27	25.1	-1.9	3.61	630.01
12:30 PM	36	37	1	1	1369

12:40 PM	40	41.6	1.6	2.56	1730.56
12:50 PM	45	50.4	5.4	29.16	2540.16
1:00 PM	57	55.4	-1.6	2.56	3069.16
1:10 P	20	24.5	4.5	20.25	600.25
1:20 PM	27	34.2	7.2	51.84	1169.64
1:30 PM	40	44.5	4.5	20.25	1980.25
1:40 PM	44	42.2	-1.8	3.24	1780.84
1:50 PM	46	46.3	0.3	0.09	2143.69
2:00 PM	55	54.4	-0.6	0.36	2959.36
TOTAL	963	977.3	14.3	169.53	42896.48
AVERAGE	38.52	39.092	0.572	6.7812	1715.859

$$RSME = \sqrt{\frac{\sum_{i=0}^{n}(T_{D\ sim} - T_{D\ exp})^2}{n}}$$

$$= \sqrt{\frac{169.52}{25}} \quad = 2.604℃$$

$$NSE = 1 - \frac{\sum_{i=0}^{n}(T_{D\ sim} - T_{D\ exp})^2}{\sum_{i=0}^{n}(T_{DSim} - \overline{T_{D\ exp}})2} = 1 - \frac{169.53}{42896.48} = 0.996$$

4.7 Validation of Simulated and the Experimental Results

The validation performance of the system as predicted by the Tansient System Simulation model (TRNSYS 16 Software) and Engineering Equation Solver (EES) was performed such that the simulation and the experimental results follow the same trends.. The validation statistical tools Root Mean Square Error (RMSE) and the Nash-Sutcliffe Coefficient (NSE) were employed to analyse the predictive power of the simulation software. The RMSE values were 4.8203^{o}C and 2.604^{o}C, while the NSE values were 0.986 and 0.996 for water temperature test. The results show little deviation of the predicted values and also a good level of fit, thereby validating the model used for simulating the solar cooker.

4.8 Analysis of the predictive power of the simulation software (TRNSYS 16) and (EES)

Table 4.1and 4.2 presented earlier show the results of statistical analysis (RMSE and NSE) employed to analyse the predictive power of the system model (TRNSYS 16) based on the simulated and experimental results.

The result of Table 4.1 shows a RMSE of 4.8203^{o}C and NSE value of 0.9867 between the model and the experimental results. This RMSE value implies that the error between the mean of the experimental water temperature and mean of simulated water temperature is 4.8203^{o}C. An NSE value of 0.9867 indicates a good quality of fit between the experimental data and the system model; hence a good model predictive power as NSE value is positive and approaches to 1 (Julien et al., 2013). Also in Table 4.2 gives the RMSE and NSE value of 2.604^{o}C and 0.996 respectively. These values as well implied the good quality of fit between the observed and simulated results. The results also indicate high predictive power of model

since the RMSE is low and the NSE value is positive and approaches to 1 (Julien et al., 2013).

4.9 System performance measurement

The evaluation of system performance was found from experimental results of 30th October, 2016 using ASAE S580 standard. The plotted results of the standardised cooking power Ps and temperature difference are shown in Figure 4.13 and 4.14 respectively.

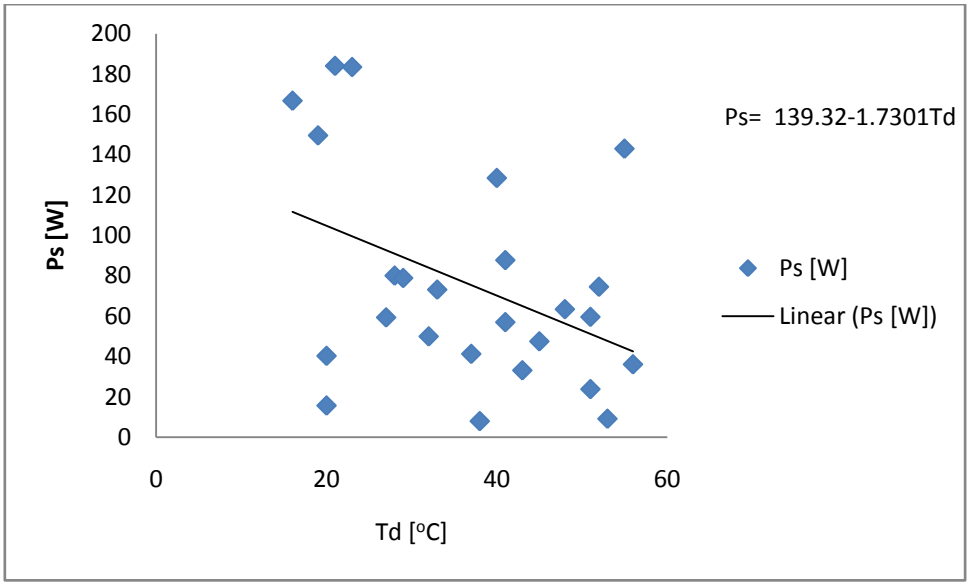


Figure 4.13: Adjusted cooking power plotted over temperature difference and resulting regression line for experimental results (30th October, 2016)

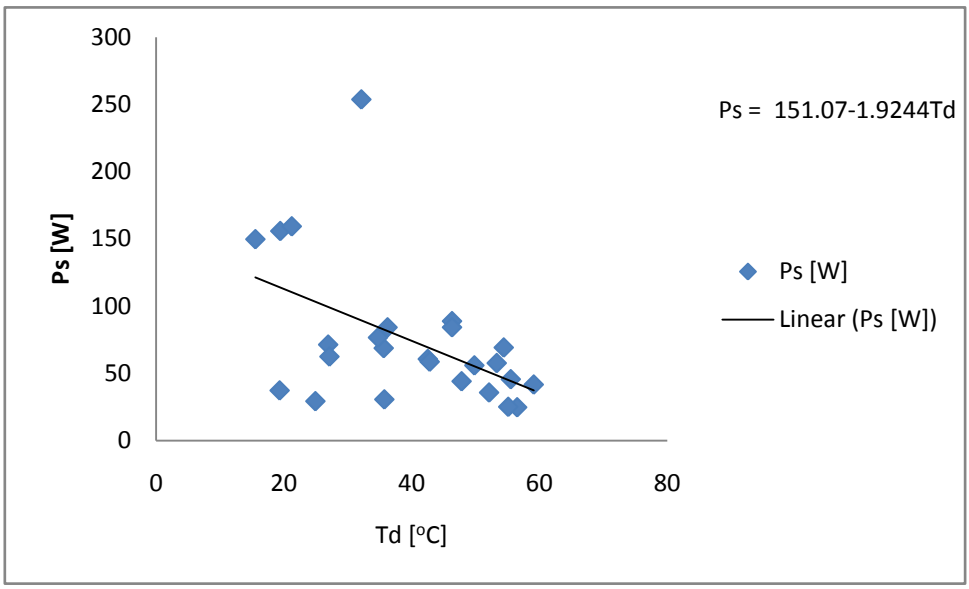


Figure 4.14: Adjusted cooking power plotted over temperature difference and resulting regression line for simulation results (30th October, 2016)

The values of standardised cooking power for a temperature difference of 50°C (ASAE S580, 2013) are computed as 52.8W and 54.8W using regression equations for the experimental and simulation results respectively.

CHAPTER FIVE

SUMMARY, CONCLUSIONS AND RECOMMENDATIONS

5.1 Summary

A solar cooker with reflectors was designed, simulated and constructed at Ahmadu Bello University Zaria, Nigeria. The system designed was modelled using TRNSYS, EES and Microsoft Excel.

At the initial stage, the typical metrological year (TMY) solar data of Zaria obtained from www.solar analytical.com was processed to obtain the monthly average daily solar resources of Zaria using the solar radiation and weather data processor TYPE 109 component of TRNSYS 16 software. The month with the least average daily solar radiation was considered as the design month. The result shows that the month of August has the least solar radiation and therefore, considered as the design month.Secondly, the solar cooker was constructed at Ahmadu Bello University, Zaria Mechanical Engineering Workshop using various tools for cutting and machining.Thirdly, the solar cooker was tested at Mechanical Engineering Department of ABU between 28^{th} and 31^{st} of October, 2016. During the course of the testing,

it was observed that in general the performance of the cooker was so encouraging because it cooked rice within an hour.Finally, the results were analysed and performance of the cooker was evaluated using (ASAE S580, 2013) standard. The cost evaluation of the system was carried out.

5.2 Conclusions

The following conclusions can be drawn:

i. A solar cooking system was designed using surface collector area 0.56m^2 and collector length of 0.8mfor Zaria metrological condition. Third reflector was added which yield 1654.6J amount of energy. The percentage energy increment was found to be 84.5%.

ii. The regression line for the experiment and simulation were obtained and were used to compute the cooking power of the cooker. The experimental and simulated cooking powers were 52.8W and 54.8W respectively. This occurred at optimum collector slope of 21^o using Zaria metrological condition.

iii. The construction of the cooker was carried out at Mechanical Engineering workshop Ahmadu Bello University Zaria. The performance evaluation was carried out where the RMSE values for 30th and 31st October, 2016 were found to be 4.8203^{o}C and 2.604^{o}C respectively. The NSE values for 30th and 31st October 2016 were found to be 0.986 and 0.996 respectively. The results show little deviation of the predicted values and also a good level of fit, thereby validating the model used for simulating the solar cooker.

5.3 Recommendations.

1. The use of various oven cavity geometries should be investigated in collector design, in order to study the effect of various geometric on the performance.

2. Alternative construction materials should be explored with a view to reduce the size and weight of the cooker for easy handling and transportation.

3. Optimisation of insulation thickness should be carried out to further minimize heat loss.

REFERENCES

Abdulwahid, B., Syed, A.Z., Zain, U.A. and Muhammad, Y.K.. (2015). Performance Modelling And Parametric Analysis of a Double Glazed Solar Oven. *Journal of Clean Energy Technology*. Vol. 4(3): pp187-191 DOI:10.7763/JOCET.2015.v4.277

Ademola, K.A. and Joseph, C.I. (2015). Energetic and Exergetic Evaluation of Box Type Solar Cooker Using Different Insulation Materials. *International Journal of Biological,Biomolecular, Agricultural Food and Bio-Technological Engineering.* Vol. 9(5): pp.426-432.

Aiden, J. (2014). Performance Evaluation of a Parabolic Solar Dish Cooker. *Journal of Applied Physics.* Vol. 5(1): pp. 46-50.

Akachukwu B.E. (2011). Prediction of Optimum Angle of Inclination of Flat Plate Solar Collector in Zaria. *Agricultural Engineering International: CIGR Journal.* Vol. 3(4)

Aremu, A.K. and Akinoso, R. (2013). Use of Solar Cooker in Nigeria. *International Food Research Journal.* Vol.20 (5): pp.2881-2886.

ASAE S580 (2013). Testing and Reporting Solar Cooker Performance. American Society of Agricultural Engineers (ASAE). The Society for Engineering in Agricultural, Food and Biological Systems. *Renewable Power Generation Committee*. 2950 Niles Road, USA.

Ashok, K. and Sudhir, C.V. (2009). Proposal for New World Standard for Testing Solar Cookers. *Journal of Engineering Science and Technology*. Vol. 4(3): pp 272-281.

Basil, O.E. (2013). Performance Evaluation of a Parabolic Solar Cooker. *International Journal of Engineering and Technology*. Vol.3 (10): pp.923-927.

Bello, A.M., Makinde, V. and Sulu, H.T. (2010). Performance Test and Thermal Efficiency, Evaluation of a Constructed Solar Box Cooker. *Journal of American Science.* Vol. 6(2): pp.32-38.

Chinnumol, F. and victor, J.(2015). A Review on Performance Improvements in Box Type Solar Cookers. *International Journal of Current Engineering and Scientific Research.* Vol. 2(7): pp. 169-175.

Dasin, D.Y. (2013). Experimental Investigations of Heat Losses from a Parabolic Concentrator Solar Cooker. *African Journal of Engineering Research.* Vol. 1(3): pp.90-96.

Duffie and Bechman (2013). Solar Engineering of Thermal Processes. John Wiley and Sons, New Jersey.

Ekechukwu, O.V.(2001). Design and Measured Performance of a Plane Reflector Augmented Box Type Solar Energy Cooker (Unpublished) thesis. Department of Mechanical Engineering, University of Nigeria, Nsukka.

Elamin, O.M. and Abdallah, I.A. (2015). Design, Construction and Performance Evaluation of Solar Cooker. *Journal of Agricultural Science and Engineering.* Vol. 1(2) pp. 75-82.

Essam A., Mohammed A., Ali, A. and Salah, A. (2010). Cylindrical Solar Cookers with Automatic Two Axes Sun Tracking System. *Jordan Journal of Mechanical andIndustrial Engineering.* Vol. 4(4): pp. 477-486.

Fabio, S. (2008). Analysis of a Flat Plate Collector on Heat and Mass Transport. Unpublished (thesis) Department of Energy Sciences. Faculty of Engineering, Lund University, Sweden.

Fumen, G.A., Aiyejagbara, E.F., Sa'id, A.I., Igbora, S.B., Musa J.J. and Philip T.K. (2014). Model Solar Box Cooker Designed for Rural Household Energy Needs. *Journal ofOccupational Safety and Environmental Health.* Vol. (2): pp. 178-183.

Goody, R. and Hu, H. (2003). Radiative Transfer/Absorption and Thermal Emission. *Journal of Heat Emission*. University of Washington, Seattle, WA, USA. pp.1859-1863.

Haftom, A., Mulu, B., kimambo, C.Z., Petros, G. and Adam, M.S. (2014). Performance Test of Parabolic Trough Solar Cooker for Indoor Cooking. *Momena Ethiopian Journal ofScience.* Vol. 6(2) pp 39-54.

Ibrahim, I.M. (2013). Design and Development of a Parabolic Dish Solar Thermal Cooker. *International of Engineering Research and Applications.* Vol. 3(4): pp. 1179-1186.

Ismail, I.R. and Isah, G. (2013). Comparative Analysis on Solar Cooking Using Box Type Solar Cooker with Finned Pot. *International Journal of Modern Engineering Research.*Vol.3(3):pp. 1290-1294.

Kulla D.M. (2011). *Technology Improvement for Safety and Economy in wood burning devices in Nigeria*, PHD thesis, Mechanical Engineering Department, Ahmadu Bello University Zaria.

Jagan, N.S. and Madhu, R.B. (2007). Thermal Performance Evaluation of Box Type Solar Cooker Using Stone Pebbles for Thermal Energy Storage. *International Journal of Renewable Energy.* Vol.2 (2): pp.11-21.

Joshua, F. (2013). Performance Evaluation of a Double-Glazed Box-Type Solar Oven with Reflector. *Journal of Renewable Energy*. Vol. 2013 (2013): Article ID 184352, 8 pages. http://dx.doi.org/10.1155/2013/184352

Julien G.A, Al-Juamily, Khalifa, N., and Yassen, T. A. (2013). Modelling solar energy transfer through roof material in Africa Sub-Saharan Regions. *ISRN Renewable Energy 34(7), 632-645.*

Lefthriotis, G. and Yianoulis, P. (2012). Glazings and Coatings. University of Patras, Grease. Elsevier Ltd.

Mohammed, B.A.(2015). Design, Simulation, Construction and Performance Evaluation of Solar Oven. (Unpublished) M.Sc dissertation. Department of Mechanical Engineering,Ahmadu Bello University, Zaria.

Medugu, D.W., Adisa, A.B., Burari, F.W. and Abdulazeez, M.A. (2013). Solar Radiation: Correlation between Measured and Predicted Values. *International Journal ofScience and Technology Education Research.* Vol.4 (1): pp. 11-17.

Mulu, B.K., John, P., Anwar, M., Asfafaw, H., Meseret, T. and Biniam, G.(2014). Theoretical and Experimental Comparison of Box Solar Cookers With and Without Internal Reflector. *Journal of Energy Procedure.*Pp: 1613 – 1622.

Neil J.S. (2010). *Encyclopedia of Research Design.* Online ISBN: 9781412961288 Publisher: SAGE Publications, Inc.

Ogunwole, O.A (2006). Flat Plate Collector Solar Cooker. *A.U. Journal of Technology.* Vol. 9(3): pp. 199-202.

Ogbuisi, N.J. (2010). *Development of Fiber Reinforced Plastic Solar cooker* (Unpublished) thesis. Department of Agricultural and Bio-Resources Engineering. University of Nigeria. Nsukka.

Rakesh K. Kaushik S.C. and Garg H.P. (1994). Analytical Study of Collector Solar Gain Enhancement by Multiple Reflectors. Centre for Energy Studies, Indian Institute of Technolgy, India. Retrieve November 2012 from http://eprint.iitd.ac.in/../kumana95.pdf

Rechard, O.H., Oliver, K. and Sarah, M.C. (2015). Efficiency Analysis of Flat Plate Collectors for Building Facade Intergration. Department of Civil Structural and Environmental Engineering. Trinity College, Dublin: Ireland.

Pranab, J., Lahkar, S.K. and Sam, D. (2010). A Review of the Thermal Performance Parameters of Box Type Solar Cookers and Identification of their Correlations. *Journal of Renewable and Sustainable Energy.*Pp 1615-1621.

Sethi, V.P, Sumathy K. and Pal D.S (2013). Optimum Inclination Angles of Booster mirrors and Solar Radiation Availabilty on the Horrizontal and Inclined Box Type Solar Cookers. *Journals of power and Energy Engineering*. Pp 53-57.

Sobamowa, M.G., Ogunmola, B.Y. and Ismail, S.O. (2012). Experimental and Numerical Investigations of Free Convection Heat Transfer in Solar Oven. *International Conference on Computational Electromagnetic.* Pp. 243-259.

Solar Cooking. (2016). Importance of Solar Cooking (April, 2016). Retrieve from http://solarcooking.com

Solar Cooker Project (2015). Jewish World Water (September 2015). Retrieve from www.solarcookerproject.org

Supple, Y.R. and Suraskar, N.N. (2012). Design and Fabrication of Manually Track Parabolic Solar Disc for In-house Cooking. *International Journal of Modern EngineeringResearch.* Vol. 2(6): pp. 4228-4230.

www.solarpoweryourhouse.com. ‘’Natural Energy and Efficient Living Solutions’’Retrieved 12 April, 2008.

www.woodsolution.com. ‘’Wood Solution Design and Build’’ Retrieved 9 July, 2016.

www.wikipedia.com. ‘’ Fibre Glass Spray Lay Up Operation’’Retrieved 28 April, 2017

Yusuf, S.O., Garba, M.M., Momoh, M. and Akpootu, D. (2014). Performance Evaluation of a Box Type Solar Oven with Reflector. *The International Journal of Engineering andScience.* Vol. 3(9): pp. 20-25.

APPENDIX A

PICTURE OF THE SOLAR COOKER



Plate A1: Thermocouple wires attached to glazing, absorber plate with pyranometer placed on the collector



Plate A2: Glazing portion of the cooker

APPENDIX B

MEASURING INSTRUMENTS



Plate B1: Solarimeter



Plate B2: Thermocouple



Plate B2: Conical flask



Plate B3: Weighing Balance

APPENDIX C

EES CODE: EVALUATION OF SOLAR COOKING TEMPERATURES

```
"Raliegh number (water)"

FUNCTION RA_w(T_s,T_infinity,L_x)
T_fl=(T_s+T_infinity)/2
beta=1/(T_fl+273)
G_r=(L_x^3*9.81*beta*(DENSITY(Water,T=T_fl,P=101.320))^2*(T_s-
T_infinity))/(VISCOSITY(Water,T=T_fl,P=101.320))^2
P_r=(CP(Water,T=T_fl,P=101.320)*1000*VISCOSITY(Water,T=T_fl,P=101.320))/COND
UCTIVITY(Water,T=T_fl,P=101.320)
R_a=G_r*P_r
RA_w=R_a
END RA_w

"Raleigh number (air)"
FUNCTION RA(T_s,T_infinity,L_x)
T_fl=(T_s+T_infinity)/2
beta=1/(T_fl+273)
G_r=(L_x^3*9.81*beta*(DENSITY(Air,T=T_fl,P=101.320))^2*(T_s-
T_infinity))/(VISCOSITY(Air,T=T_fl))^2
P_r=(CP(Air,T=T_fl)*1000*VISCOSITY(Air,T=T_fl))/CONDUCTIVITY(Air,T=T_fl)
R_a=G_r*P_r
RA=R_a
END RA


FUNCTION TEMP(row, T_abt)
IF row=1 then T_as:=T_abt ELSE T_as=TableValue('Table 1',row-1,2)
TEMP:=T_as
END

"Water temperature"
T_io_old=TEMP(row, T_a)
row=Time/delta+1
delta=600

"HEAT BALANCE EQUATIONS"
U_t*(T_a-T_c)+h_r*(T_p-T_c)+h_a*(T_io-T_c)=0  "cover"
A_c*S+A_sb*U_sb*(T_a-T_p)+(A_sb*h_a)*(T_io-T_p)+A_c*h_r*(T_c-T_p)=0 "absorber"
```

```
A_c*h_a*(T_c-T_io)+(A_sb*h_a)*(T_p-T_io)+0.24*h_t*(T_t-T_io)+0.12426*h_pt*(T_pt-T_io)=0 "air"
0.24*h_t*(T_io-T_t)+6300*(T_pt-T_t)=0  "tray"
6300*(T_t-T_pt)+0.12426*h_pt*(T_io-T_pt)+0.06*h_wt*(T_f-T_pt)=0  "pot"
q_u=0.06*h_wt*(T_pt-T_f) "water"
q_u=m*c*(T_f-T_io_old)/t

t=600;
“Area of side and bottom”
A_sb=A_c+4*d*sqrt(A_c);
m=1.6; c=4190;A_c=0.49;d=0.3;

"Convective heat transfer coefficient of water (h_wt)"
N_u_wt=0.68+0.67*R_a_wt^(1/4)/(1+(0.492/P_r_wt)^(9/16))^(4/9)

P_r_wt=(CP(Water,T=(T_f+T_io)/2,P=101.320)*1000*VISCOSITY(Water,T=T_f,P=101.320))/CONDUCTIVITY(Water,T=T_f,P=101.320)

R_a_wt=RA_w(T_io,T_f,0.3)

h_wt=N_u_wt*CONDUCTIVITY(Water,T=T_f,P=101.320)/0.3

"Convective heat transfer coefficient of air (h_a)"
N_u_a=0.52*(RA_a)^(1/4)
h_a=(N_u_a*CONDUCTIVITY(Air,T=T_io))/1.3
"h_a=(0.061*CONDUCTIVITY(Air,T=T_io)*(RA_a)^(1/3))/d"
RA_a=RA(T_p,T_io,1.3)

"Radiative heat transfer coefficient of air (h_r)"
h_r=(4*sigma#*(T_io+273)^3)/((1/e_1)+(1/e_2)-1)
e_1=0.88; e_2=0.95;
" Top loss coefficient (U_t)"
U_t=h_w+h_r_c_a ;     V=0.2

"Radiation coefficient of cover to air (h_c_r_a)"
h_r_c_a=e_1*sigma#*((T_c+273)^2+(T_a+273)^2)*(T_c+T_a+546)

"Wind heat transfer coefficient (h_w)"
h_w=5.7+3.8*V

" Side and bottom loss coefficient (U_sb)"
U_sb=1/(x_1/k_1+x_i/k_i+x_2/k_2)

"Convective heat transfer coefficient of pot (h_pt)"
```

N_u_pt=0.52*(RA_pt)^(1/4)
h_pt=(N_u_pt*CONDUCTIVITY(Air,T=T_io))/0.1
"h_a=(0.061*CONDUCTIVITY(Air,T=T_io)*(RA_a)^(1/3))/d"
RA_pt=RA(T_io,T_pt,0.1)
x_1=0.015; x_2=0.015; x_i=0.1; k_1=0.2; k_2=0.2; k_i=0.06

"Convective heat transfer coefficient of tray (h_t)"
N_u_t=0.52*(RA_t)^(1/4)
h_t=(N_u_t*CONDUCTIVITY(Air,T=T_io))/0.6
"h_a=(0.061*CONDUCTIVITY(Air,T=T_io)*(RA_a)^(1/3))/d"
RA_t=RA(T_io,T_t,0.6)

APPENDIX D

EXPERIMENTAL RESULTS

Table 1: Experimental Result for stagnation temperature test for 28th October, 2016

Time [min]	To [^oC]	Tam [^oC]	I [W/m^2]	Tg1 [^oC]	Tg2 [^oC]	Tap [^oC]	Tm [^oC]	η_{cexp}
10:00 AM	69	28	728	40	63	65	48.5	0.73920
10:10 AM	72	29	811	42	71	69	50.5	0.74744
10:20 AM	78	29	853	43	79	74	53.5	0.73638
10:30 AM	81	30	870	49	83	76	55.5	0.73344
10:40 AM	83	30	895	51	86	79	56.5	0.73195
10:50 AM	86	32	910	53	89	83	59	0.73164
11:00 AM	89	33	932	55	94	87	61	0.72978
11:10 AM	93	33	944	61	97	89	63	0.72110
11:20 AM	97	34	986	61	99	92	65.5	0.72026
11:30 AM	102	34	992	61	103	94	68	0.70862
11:40 AM	106	35	1002	62	106	99	70.5	0.70285
11:50 AM	109	35	1009	62	108	104	72	0.69665
12:00 PM	111	35	1060	69	108	109	73	0.70075
12:10 PM	113	35	1071	71	109	113	74	0.69792
12:20 PM	119	31	1077	71	109	119	75	0.67572
12:30 PM	121	31	1080	71	110	122	76	0.67166
12:40 PM	125	32	998	72	110	124	78.5	0.64703
12:50 PM	129	32	956	72	115	124	80.5	0.62633
1:00 PM	132	33	955	71	115	127	82.5	0.62083
1:10 PM	136	32	972	71	116	129	84	0.61251
1:20 PM	136	32	980	72	116	133	84	0.61469
1:30 PM	141	33	972	74	119	136	87	0.60222
1:40 PM	142	34	932	76	119	141	88	0.5903
1:50 PM	142	34	921	80	120	144	88	0.58684
2:00 PM	141	35	901	81	121	143	88	0.58588
Total	2753	811	23807	1591	2565	2675	1782	16.932
Average	110.12	32.44	952.28	63.64	102.6	107	71.28	0.6772

Table 2: Experimental results (load test) using 1.6kg of water and 0.35kg of rice for 29th October, 2016

Time [min]	T_w [^oC]	T_a [^oC]	I [W/m^2]	T_{g1} [^oC]	T_{g2} [^oC]	T_{ap} [^oC]
10:00 AM	48	27	625	37	61	64
10:10 AM	59	27	711	41	69	68
10:20 AM	68	27	713	44	75	72
10:30 AM	79	28	741	48	78	74
10:40 AM	87	28	792	52	84	79
10:50 AM	91	28	804	54	89	83
11:00 AM	51	29	934	56	91	89
11:10 AM	67	29	936	60	93	91
11:20 AM	78	29	939	60	97	95
11:30 AM	86	30	942	62	101	99
11:40 AM	90	30	986	64	104	101
11:50 AM	53	31	998	67	107	108
12:00 PM	64	31	1062	72	111	112
12:10 PM	77	31	1074	72	112	117
12:20 PM	83	32	1081	73	112	119
12:30 PM	91	33	1090	73	116	122
12:40 PM	54	33	1080	75	116	126
12:50 PM	69	34	1020	76	117	129
1:00 PM	78	34	991	76	120	131
1:10 PM	85	34	982	78	120	133
1:20 PM	90	35	972	79	121	136
1:30 PM	55	35	941	81	120	139
1:40 PM	67	34	939	82	122	142
1:50 PM	79	35	920	83	122	144
2:00 PM	88	35	910	82	121	145
Total	1837	779	23183	1647	2579	2718
Average	73.48	31.16	927.32	65.88	103.16	108.72

Table 3: Experimental Result for load test (water) on 30th October, 2016

Tam [°C]	I [W/m^2]	Tg1 [°C]	Tg2 [°C]	Tap [°C]	Td [°C]	Ps [W]
28	750	38	60	63	16	166.6944
28	776	42	65	67	20	40.27732
28	781	45	69	70	28	80.03892
29	791	47	74	73	40	128.419
29	823	53	79	76	45	47.47145
30	839	58	81	79	52	74.50584
30	866	59	83	84	56	36.09145
30	892	61	86	86	21	183.9572
31	922	61	89	90	27	59.32386
32	939	63	92	94	32	49.92843
32	947	63	96	98	37	41.25554
32	983	65	98	103	38	7.948932
33	984	69	106	107	55	142.9354
33	993	72	109	111	19	149.5088
34	998	74	112	113	20	15.65892
35	991	74	114	117	29	78.84763
34	980	74	114	120	41	87.70592
35	986	76	117	121	48	63.39797
35	985	76	118	125	51	23.79838
36	980	77	118	127	23	183.3851
35	962	79	119	130	33	73.10208
34	960	79	119	134	41	56.97563
36	944	80	120	137	43	33.10932
35	918	81	120	139	51	59.58235
34	857	82	122	141	53	9.11762
808	22847	1648	2480	2605	919	1893.037
32.32	913.88	65.92	99.2	104.2	36.76	75.72149

Table 4: Experimental Result for load test on 31st October, 2016

Time [min]	Tw [°C]	Tam [°C]	I [W/m2]	Tg1 [°C]	Tg2 [°C]	Tap [°C]	Td [C]	Ps [W]
10:00 AM	46	29	772	43	58	62	17	172.065
10:10 AM	47	29	791	46	62	68	18	9.87838
10:20 AM	59	29	804	48	67	73	30	116.623
10:30 AM	68	30	825	51	72	74	38	85.2414
10:40 AM	79	30	874	53	75	78	49	98.3430
10:50 AM	86	30	930	55	80	82	56	58.8135
11:00 AM	88	31	939	62	84	85	57	16.6428
11:10 AM	49	31	950	66	87	88	18	148.050
11:20 AM	55	31	842	69	91	92	24	55.6802
11:30 AM	69	31	851	69	92	93	38	128.546
11:40 AM	76	32	869	71	97	97	44	62.942
11:50 AM	86	32	899	71	107	101	54	86.9165
12:00 PM	90	32	965	72	110	105	58	32.3888
12:10 PM	57	32	971	72	114	109	25	201.179
12:20 PM	60	33	988	74	117	114	27	23.7261
12:30 PM	69	33	1027	74	118	116	36	68.4753
12:40 PM	74	34	1007	74	118	119	40	38.7974
12:50 PM	79	34	743	76	119	122	45	52.5827
1:00 PM	91	34	874	76	119	127	57	107.283
1:10 PM	53	33	941	76	120	131	20	166.074
1:20 PM	61	34	931	79	120	133	27	67.1432
1:30 PM	74	34	927	79	120	138	40	109.578
1:40 PM	78	34	924	80	121	141	44	33.8259
1:50 PM	81	34.2	920	81	120	143	46	25.4797
2:00 PM	90	34.3	890	80	122	143	55	79.0159
Total	1765	800.5	22454	1697	2510	2634	963	2045.29
Average	70.6	32.02	898.16	67.88	100.4	105.36	38.52	81.8118

Table 5: Average solar intensity with time from 28/10/2016 to 31/10/2016

Time [min]	Day 1	Day 2	Day 3	Day 4	Average
10:00 AM	728	625	750	772	718.75
10:10 AM	811	711	776	791	772.25
10:20 AM	853	713	781	804	787.75
10:30 AM	870	741	791	825	806.75
10:40 AM	895	792	823	874	846
10:50 AM	910	804	839	930	870.75
11:00 AM	932	934	866	939	917.75
11:10 AM	944	936	892	950	930.5
11:20 AM	986	939	922	842	922.25
11:30 AM	992	942	939	851	931
11:40 AM	1002	986	947	869	951
11:50 AM	1009	998	983	899	972.25
12:00 PM	1060	1062	984	965	1017.75
12:10 PM	1071	1074	993	971	1027.25
12:20 PM	1077	1081	998	988	1036
12:30 PM	1080	1090	991	1027	1047
12:40 PM	998	1080	980	1007	1016.25
12:50 PM	956	1020	986	743	926.25
1:00 PM	955	991	985	874	951.25
1:10 PM	972	982	980	941	968.75
1:20 PM	980	972	962	931	961.25
1:30 PM	972	941	960	927	950
1:40 PM	932	939	944	924	934.75
1:50 PM	921	920	918	920	919.75
2:00 PM	901	910	857	890	889.5

APPENDIX E

SIMULATION RESULTS

Table 6: Simulated Result for stagnation temperature test for 28th October, 2016

Time [min]	To [^oC]	Tam [^oC]	I [W/m^2]	Tm [^oC]	η_{csim}
10:00 AM	65.2	31.2	816	48.2	0.775833
10:10 AM	70.4	31.6	845	51	0.765207
10:20 AM	75.6	31.9	872	53.75	0.754713
10:30 AM	79.2	32.1	898	55.65	0.748875
10:40 AM	81.7	32.8	923	57.25	0.747551
10:50 AM	84.6	32.9	945	58.75	0.743228
11:00 AM	87.7	33.2	965	60.45	0.738808
11:10 AM	91.3	33.5	982	62.4	0.732851
11:20 AM	96.4	33.7	998	65.05	0.722936
11:30 AM	100.7	33.9	1010	67.3	0.714653
11:40 AM	103.4	34.2	1020	68.8	0.710392
11:50 AM	107.7	34.6	1030	71.15	0.702573
12:00 PM	110.8	34.8	1040	72.8	0.697308
12:10 PM	112.2	35.1	1040	73.65	0.694663
12:20 PM	118.8	35.3	1050	77.05	0.68119
12:30 PM	122.3	35.4	1040	78.85	0.671106
12:40 PM	123.7	35.6	1030	79.65	0.666165
12:50 PM	126.6	35.9	1030	81.25	0.659854
1:00 PM	128.1	35.9	1020	82	0.65402
1:10 PM	133.7	34.2	1010	83.95	0.633713
1:20 PM	134.2	34.3	999	84.25	0.63
1:30 PM	137.4	34.6	986	86	0.619351
1:40 PM	140.4	34.8	969	87.6	0.607554
1:50 PM	140.8	35.2	952	88	0.602689
2:00 PM	140.9	35.7	932	88.3	0.597811
Total	2713.8	852.4	24402	1783.1	17.27305
Average	108.552	34.096	976.08	71.324	0.690922

Table 7: Simulated Result for load test on 30th October, 2016

Time [min]	Tw [^{o}C]	Tam [^{o}C]	I [W/m^{2}]	Td [^{o}C]	Ps [W]
10:00 AM	45.6	30.1	809	15.5	149.7082
10:10 AM	49.6	30.3	838	19.3	37.29737
10:20 AM	57.5	30.6	865	26.9	71.36303
10:30 AM	67.1	30.9	891	36.2	84.18909
10:40 AM	77.5	31.2	915	46.3	88.81259
10:50 AM	85.8	31.4	937	54.4	69.21509
11:00 AM	90.9	31.8	956	59.1	41.6845
11:10 AM	51.8	32.4	973	19.4	155.7942
11:20 AM	59.7	32.6	988	27.1	62.47877
11:30 AM	68.5	32.9	1000	35.6	68.76144
11:40 AM	79.5	33.2	1020	46.3	84.26647
11:50 AM	87.1	33.8	1030	53.3	57.65522
12:00 PM	90.4	33.9	1040	56.5	24.79379
12:10 PM	55.3	34.1	1040	21.2	159.2813
12:20 PM	59.2	34.3	1040	24.9	29.30175
12:30 PM	69.4	34.7	1040	34.7	76.63535
12:40 PM	77.4	34.9	1030	42.5	60.68971
12:50 PM	84.7	34.9	1020	49.8	55.92229
1:00 PM	90.6	35.1	1010	55.5	45.64497
1:10 PM	67.3	35.2	989	32.1	253.6127
1:20 PM	71.1	35.4	969	35.7	30.64235
1:30 PM	78.2	35.4	946	42.8	58.6448
1:40 PM	83.4	35.6	921	47.8	44.117
1:50 PM	87.5	35.4	896	52.1	35.75511
2:00 PM	90.3	35.2	871	55.1	25.11899
Total	1825.4	835.3	24034	990.1	1871.386
Average	73.016	33.412	961.36	39.604	74.85544

Table 8: Simulated Result for load test on 31st October, 2016

Time [min]	Tw [^{o}C]	Tam [^{o}C]	I [W/m^{2}]	Td [^{o}C]	Ps [W]
10:00 AM	47.1	31.1	809	16	154.5375
10:10 AM	48.1	31.3	839	16.8	9.31323
10:20 AM	59.4	31.7	866	27.7	101.9584
10:30 AM	74.6	32.1	893	42.5	133.0009
10:40 AM	80.3	32.4	918	47.9	48.51706
10:50 AM	88.2	32.7	940	55.5	65.66917
11:00 AM	90.7	33.2	960	57.5	20.34844
11:10 AM	52.3	33.9	977	18.4	147.1586
11:20 AM	57.4	33.9	992	23.5	40.17175
11:30 AM	70.6	34.1	1010	36.5	102.121
11:40 AM	78.8	34.6	1020	44.2	62.81682
11:50 AM	87.4	34.8	1030	52.6	65.24144
12:00 PM	92.4	34.9	1030	57.5	37.93107
12:10 PM	60.2	35.1	1040	25.1	188.5831
12:20 PM	60.4	35.3	1040	25.1	1.502654
12:30 PM	72.4	35.4	1040	37	90.15923
12:40 PM	77.2	35.6	1040	41.6	36.06369
12:50 PM	86.2	35.8	1020	50.4	68.94529
1:00 PM	91.3	35.9	1020	55.4	39.069
1:10 PM	59.5	35	1010	24.5	189.5427
1:20 PM	69.4	35.2	996	34.2	77.66729
1:30 PM	77.8	35.4	983	44.5	66.77103
1:40 PM	79.9	35.6	967	42.2	16.96896
1:50 PM	82.1	35.8	949	46.3	18.11418
2:00 PM	90.3	35.9	930	54.4	68.89587
Total	1834	856.7	24319	977.3	1851.068
Average	73.36	34.268	972.76	39.092	74.04272

APPENDIX F

VERSION 16.1

****
****

*** TRNSYS input file (deck) generated by TrnsysStudio

*** on Sunday, November 27, 2016 at 09:27

*** fromTrnsysStudio project:
C:\PROGRA~1\TRNSYS~1\MyProjects\Project35\Project35.tpf

***

*** If you edit this file, use the File/Import TRNSYS Input File function in

*** TrnsysStudio to update the project.

***

*** If you have problems, questions or suggestions please contact your local

*** TRNSYS distributor or mailto:software@cstb.fr

***

****
****

****
****

*** Units

****
****

****
****

*** Control cards

****
****

* START, STOP and STEP

```
CONSTANTS 3
START=7200
STOP=7224
STEP=0.166666666666667
* User defined CONSTANTS
SIMULATION	START	STOP	STEP	! Start time	End time	Time step
TOLERANCES 0.001 0.001			! Integration	Convergence
LIMITS 30 30 30			! Max iterations	Max warnings Trace limit
DFQ 1			! TRNSYS numerical integration solver method
WIDTH 80			! TRNSYS output file width, number of characters
LIST			! NOLIST statement
			! MAP statement
SOLVER 0 1 1			! Solver statement	Minimum relaxation factor	Maximum relaxation factor
NAN_CHECK 0			! Nan DEBUG statement
OVERWRITE_CHECK 0			! Overwrite DEBUG statement
TIME_REPORT 0			! disable time report
EQSOLVER 0			! EQUATION SOLVER statement
* Model "Zaria weather" (Type 109)
UNIT 3 TYPE 109	Zaria weather
*$UNIT_NAME Zaria weather
*$MODEL .\Weather Data Reading and Processing\Standard Format\TMY2\Type109-TMY2.tmf
*$POSITION 211 218
*$LAYER Weather - Data Files #
PARAMETERS 4
2		! 1 Data Reader Mode
30		! 2 Logical unit
```

4 ! 3 Sky model for diffuse radiation

1 ! 4 Tracking mode

INPUTS 5

0,0 ! [unconnected] Ground reflectance

0,0 ! [unconnected] Slope of surface-1

0,0 ! [unconnected] Azimuth of surface-1

0,0 ! [unconnected] Slope of surface-2

0,0 ! [unconnected] Azimuth of surface-2

*** INITIAL INPUT VALUES

0.2 21 0.0 90 0.0

*** External files

ASSIGN "C:\Users\SHEIK\Desktop\Solar Oven\SOLAR LIB\Zaria_Nigeria_SPtMasterTable_472122_19790101_20100101_tmy2.tm2" 30

*|? Weather data file |1000

*--

* EQUATIONS "Absorbed Energy"

*

EQUATIONS 15

R = 0.8

beta = 21

alpha_n = 30

alpha_s = 0

F_n = min(F_n1,F_n2)

F_s = min(F_s1,F_s2)

F_n1 = R*cos([3,16]+alpha_n)

F_n2 = R*sin(beta+[3,16]+(2*alpha_n)-(11/2))

F_s1 = R*sin([3,16]-alpha_s)

```
F_s2 = R*cos(beta+[3,16]-(2*alpha_s))
Q = tau*alpha*(A_c*[3,18]+A_r*F_s*[3,25])*(1000/3600)
A_c = 0.48
A_r = 0.63
tau = 0.8
alpha = 0.9
*$UNIT_NAME Absorbed Energy
*$LAYER Main
*$POSITION 419 84
*------------------------------------------------------------------------
* Model "Type25c" (Type 25)
UNIT 8 TYPE 25       Type25c
*$UNIT_NAME Type25c
*$MODEL .\Output\Printer\Unformatted\No Units\Type25c.tmf
*$POSITION 599 226
*$LAYER Outputs #
PARAMETERS 10
STEP          ! 1 Printing interval
START                 ! 2 Start time
STOP          ! 3 Stop time
31            ! 4 Logical unit
0             ! 5 Units printing mode
0             ! 6 Relative or absolute start time
-1            ! 7 Overwrite or Append
-1            ! 8 Print header
0             ! 9 Delimiter
1             ! 10 Print labels
```

```
INPUTS 3
5,3             ! Type55:Mean value of input ->Input to be printed-1
I_conv          ! Equa:I_conv ->Input to be printed-2
T_am            ! Equa:T_am ->Input to be printed-3
*** INITIAL INPUT VALUES
T I T_am
*** External files
ASSIGN "C:\Users\SHEIK\Desktop\conv.txt" 31
*|? Output file for printed results |1000
*-------------------------------------------------------------------------
* Model "Type55" (Type 55)
UNIT 5 TYPE 55       Type55
*$UNIT_NAME Type55
*$MODEL .\Utility\Integrators\Periodic Integrator\Type55.tmf
*$POSITION 596 71
*$LAYER Main #
PARAMETERS 7
-1              ! 1 Integrate or sum input
1               ! 2 Relative starting hour for input
24              ! 3 Duration for input
0.16666666666666666667          ! 4 Cycle repeat time for input
0.16666666666666666667          ! 5 Reset time for input
0               ! 6 Absolute starting hour for input
8760            ! 7 Absolute stopping hour for input
INPUTS 1
Q               ! Absorbed Energy:Q ->Input
*** INITIAL INPUT VALUES
```

```
0.
*-------------------------------------------------------------------------
* Model "Type65d" (Type 65)
UNIT 6 TYPE 65        Type65d
*$UNIT_NAME Type65d
*$MODEL .\Output\Online Plotter\Online Plotter Without File\Type65d.tmf
*$POSITION 733 58
*$LAYER Main #
PARAMETERS 12
2               ! 1 Nb. of left-axis variables
2               ! 2 Nb. of right-axis variables
0.0             ! 3 Left axis minimum
1000.0          ! 4 Left axis maximum
0.0             ! 5 Right axis minimum
1000.0          ! 6 Right axis maximum
1               ! 7 Number of plots per simulation
12              ! 8 X-axis gridpoints
0               ! 9 Shut off Online w/o removing
-1              ! 10 Logical unit for output file
0               ! 11 Output file units
0               ! 12 Output file delimiter
INPUTS 4
5,3             ! Type55:Mean value of input ->Left axis variable-1
0,0             ! [unconnected] Left axis variable-2
0,0             ! [unconnected] Right axis variable-1
0,0             ! [unconnected] Right axis variable-2
*** INITIAL INPUT VALUES
```

Mean Q label label

LABELS 3

"Temperatures"

"Heat transfer rates"

"Graph 1"

*----------

* EQUATIONS "Equa"

EQUATIONS 2

I_conv = [3,18]*(1000/3600)

T_am = [3,1]

*$UNIT_NAME Equa

*$LAYER Main

*$POSITION 416 324

*----------

END